Geological Society of America Bulletin, published online on 3 May 2012 as doi:10.1130/B30576.1

Geological Society of America Bulletin

Petrology of the Grays River volcanics, southwest Washington: Plume-influenced slab window magmatism in the Cascadia forearc

Christine F. Chan, Jeffrey H. Tepper and Bruce K. Nelson

Geological Society of America Bulletin published online 3 May 2012;
doi: 10.1130/B30576.1

Geological Society of America Bulletin, published online on 3 May 2012 as doi:10.1130/B30576.1

Petrology of the Grays River volcanics, southwest Washington: Plume-influenced slab window magmatism in the Cascadia forearc

Christine F. Chan[1,*,†], Jeffrey H. Tepper[1,†], and Bruce K. Nelson[2,†]
[1]*Geology Department, University of Puget Sound, Tacoma, Washington 98416-1048, USA*
[2]*Department of Earth and Space Sciences, 351310, University of Washington, Seattle, Washington 98195, USA*

ABSTRACT

The Grays River volcanics are part of the Coast Range basalt province and consist of ~3500 m of tholeiitic basalt flows and volcaniclastic rocks that erupted in the Cascadia forearc from 42 to 37 Ma. Chemical and isotopic data, combined with migration of the location of magmatism through time, indicate that Grays River volcanics magmatism was related to subduction of a plume-influenced spreading ridge that produced a northward-migrating slab window. Involvement of a mantle plume source is indicated by ocean-island basalt (OIB)–like incompatible element enrichments and radiogenic Pb isotopic compositions ($^{206}Pb/^{204}Pb > 19.3$). These Pb isotope data are distinct from most Cascade arc rocks and from Cascadia sediment, but they overlap with compositions of other Coast Range basalts. A slab window setting accounts for the northward-younging age progression of the Grays River volcanics as well as geochemical traits, including low B/Be, that indicate the Grays River magmas ascended through the mantle wedge and subducting slab without acquiring an arc signature. Differentiation of Grays River magmas was dominated by clinopyroxene fractionation, which resulted in evolved compositions (Mg# = 59–32), low Sc contents, and Sr contents that increase with fractionation. Geochemical differences between the Grays River volcanics and other Cascadia forearc volcanic units that range from ca. 55 Ma (Crescent Basalts) to <3 Ma (Boring Lavas) were mainly caused by transient changes in tectonic setting (i.e., arrival of a mantle plume, ridge subduction) and do not record progressive chemical modification of the mantle wedge.

*Current address: Department of Geosciences, Oregon State University, Corvallis, Oregon 97331-5506, USA.

†E-mails: chanchr@geo.oregonstate.edu; jtepper@pugetsound.edu; bnelson@uw.edu

INTRODUCTION

Although the forearc region of a convergent plate margin is generally associated with low heat flow and a lack of igneous activity (Gill, 1981), many continental and island-arc systems preserve a record of forearc magmatism. Magmas produced in this setting are generally small in volume but diverse in composition, ranging from basalts with mid-ocean-ridge (MORB) or ocean-island (OIB) traits (Kimura et al., 2005) to adakites (Benoit et al., 2002), boninites and high-Mg andesites (Deschamps and Lallemand, 2003), and a variety of felsic rocks (Madsen et al., 2006). Mechanisms proposed to account for forearc magmatism are also diverse, the most common being subduction of a spreading ridge (Madsen et al., 2006), rifting of the overriding plate (Davis et al., 1995), breakoff of the downgoing plate (Schoonmaker et al., 2005), magma leakage along transform faults (Gill, 1981), and the presence of a mantle plume (MacPherson and Hall, 2001). Because forearc igneous rocks record events and processes operating at the entryway to a subduction zone, they are particularly useful for understanding subduction processes as well as for reconstructing plate motions and geometries. Determining their origin(s) in any particular locality thus has both tectonic and petrologic importance.

In the Pacific Northwest the Early Tertiary was a time of widespread and diverse volcanism in a rapidly changing tectonic setting. Plate reorganization in the North Pacific between 61 and 48 Ma led to decreasing convergence rates between the Kula-Farallon and North American plates (Wells et al., 1984). Several spreading ridges, including the Kula-Farallon, Resurrection-Farallon, and Pacific-Farallon, intersected the continental margin during this time, producing multiple slab windows that migrated along the Cascadia margin (Babcock et al., 1992; Haeussler et al., 2003; Madsen et al., 2006). At the same time, voluminous, dominantly basaltic volcanism occurred along the continental margin from southern Oregon to Vancouver Island and continued until after establishment of the modern Cascade arc at ca. 40 Ma (Babcock et al., 1992). At least three tectonic models have been proposed to explain this mafic continental margin magmatism: (1) hotspot volcanism centered on a spreading ridge that was later accreted (Duncan, 1982), (2) oblique rifting of the continental margin (Wells et al., 1984; Snavely, 1987), and (3) passage of a slab window related to ridge subduction (Babcock et al., 1992).

The focus of this study is on the 42–37 Ma Grays River volcanics, the northernmost of several late Eocene, dominantly basaltic volcanic units in the Coast Range of Washington and Oregon. Based on major-element, trace-element, and Sr-Nd-Pb isotope compositions of the Grays River volcanics, we present a model that describes: (1) the tectonic setting in which these forearc magmas were generated, (2) the nature of their mantle source(s), and (3) the processes responsible for their compositional diversity.

Cascadia also affords an opportunity to examine the changing character of forearc magmatism through time. The Crescent Formation (ca. 54–48 Ma) and other early Eocene basalts of Siletzia represent forearc volcanism associated with low-angle subduction of the Farallon plate prior to establishment of the modern Cascade arc. These were followed by the Grays River volcanics (42–37 Ma), which span the interval from just before to ~3 m.y. after initiation of the modern arc. Most recently, the Boring Lavas, which erupted in and around the Portland Basin from 3.0 to 0.5 Ma, represent volcanism after the arc was well established. By comparing chemical and isotopic traits of these three units, which erupted in close proximity over a span of more than 50 m.y., we can evaluate how and why forearc magmatism changes as an arc matures.

GEOLOGIC SETTING AND PREVIOUS WORK

From Oregon to Vancouver Island, the Paleogene geology of the Cascadia forearc region is dominated by thick accumulations of Lower to

GSA Bulletin; doi: 10.1130/B30576.1; 9 figures; 3 tables; Data Repository item 2012170.

Middle Eocene submarine and subaerial basalts that are overlain by Middle to Upper Eocene sedimentary rocks (Snavely and Wells, 1996). The basalts, which are interbedded with continental margin sediments in a series of basins, have individual formation names (Roseburg, Siletz River, Crescent, and Metchosin) but are collectively known as Siletzia (Fig. 1). Seismic profiling data indicate these basalts are >30 km thick in some areas and form the basement for much of the forearc region (Trehu et al., 1994). Based on their mix of MORB and OIB geochemical traits, great stratigraphic thickness, association with continentally derived conglomerates, and northward-younging age progression, Siletzia basalts have been attributed to volcanism in a series of marginal rift basins that developed in response to subduction of the Kula-Farallon spreading ridge (Babcock et al., 1992). Other workers have interpreted Siletzia as a hotspot chain (Duncan, 1982) or oceanic plateau (Wells, 2007) that formed offshore and was subsequently accreted to the margin, and Pyle et al. (2009) suggested that these basalts represent the plume-head phase of the Yellowstone hotspot. These hotspot models are consistent with the isotopic compositions, large volume, and restricted age range of Siletzia basalts, but they are less satisfactory for explaining why volcanism migrated northward along the margin during a time when North America was moving westward relative to a hotspot frame of reference (Engebretson et al., 1985).

Beginning ca. 50 Ma, following emplacement of the Siletzia basalts, the convergence rate between the North American and Farallon plates decreased (Verplank and Duncan, 1987). This shift has been linked to accretion of a thick basalt section, which was too buoyant to subduct and may have caused the subduction zone to jump westward and steepen, leading to establishment of the modern Cascade arc at ca. 42 Ma (Wells et al., 1984). During the 50–38 Ma time interval, changes in plate motions also resulted in differential rotation of small, discrete crustal blocks within the Washington and Oregon Coast Ranges and development of northwest-trending conjugate faults in southwest Washington (Wells and Coe, 1985; Armentrout, 1987). Paleomagnetic data suggest individual blocks experienced 30°–75° of clockwise rotation (Simpson and Cox, 1977; Wells and Coe, 1985). Crustal extension during the middle Eocene trigged rapid subsidence of the basement rocks, resulting in formation of a forearc basin that extended 640 km from southern Vancouver Island to the Klamath Mountains of southwestern Oregon (Niem and Niem, 1984; Niem et al., 1992a).

Following the cessation of Siletzia volcanism at ca. 45 Ma (Pyle et al., 1997), the Cascadia forearc region experienced two episodes of less voluminous, late Eocene volcanism: 47–43 Ma adakitic volcanism on the Olympic Peninsula (Wolfe and Tepper, 2004) and ca. 46–32 Ma dominantly basaltic volcanism in the Oregon and southern Washington Coast Ranges. Units included in the latter are, from south to north, the Yachats Basalt and the Basalt of Cascade Head (Davis et al., 1995; Parker et al., 2010), various small alkalic intrusions (Oxford, 2006), the Tillamook volcanics (Magill et al., 1981), the Goble volcanics (Beck and Burr, 1979), and the Grays River volcanics, which are the subject of this paper. The majority of these mafic eruptive centers were subaerial, and they subdivided the forearc basin into smaller marginal basins that subsequently filled with slope mudstones and turbidite sandstones (Niem et al., 1992b; Moothart, 1992).

Early studies grouped the Grays River volcanics together with the 37–34 Ma Goble volcanics (Henriksen, 1956; Livingston, 1966; Wolfe and McKee, 1968; Wells, 1981) until Phillips (1987) recognized that the two units were chemically distinct. Subsequently, the Grays River volcanics were the focus of a series of Oregon State University Master of Science (M.S.) theses that emphasized structure, stratigraphy, geochronology, and paleomagnetic studies, their goal in part being to better understand nearby natural gas fields (Rarey, 1985; Mumford, 1988; Safley, 1989; Moothart, 1993; Kleibacker, 2001; Eriksson, 2002; McCutcheon, 2004).

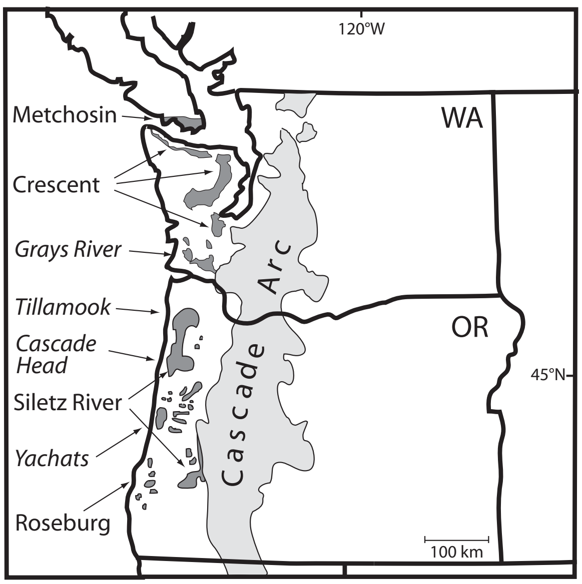

Figure 1. Simplified geologic map of the Cascadia forearc region showing the distribution of Coast Range basalt units in relation to rocks of the Cascade arc (after Wells et al., 1984; Babcock et al., 1992). The names of late Eocene Coast Range units are italicized.

Grays River Volcanics—Age and Field Relations

The Grays River volcanics consist of nearly 3500 m of basaltic lava flows and volcaniclastic rocks (McCutcheon, 2003) that range in age from 41.4 to 36.8 Ma (Kleibacker, 2001). Ar-Ar dates for eight samples (Fig. 2; GSA Data Repository material[1]) reveal a general younger-to-the-northeast age progression (Payne, 1998) (Fig. 2). A date from Mount Solo (sample M04, south of Rocky Point in Fig. 2) does not fit the age trend; this sample is also anomalously young given its stratigraphic position below the Cowlitz Formation and may be an invasive flow (McCutcheon, 2003). An intraformational unconformity separates the Grays River volcanics into a lower and an upper unit. The lower unit (41.4 to ca. 39 Ma; Kleibacker, 2001) is ~1250 m thick and consists of tholeiitic pillow basalts, submarine hyaloclastites, and some subaerial flows. The upper unit (38.6–36.8 Ma; Kleibacker, 2001), typically ~150 m thick, though in some areas up to 300 m thick, is composed of subaerial basaltic andesite to dacitic flows (Rarey, 1985; Mumford, 1988). In summary, the two subunits are petrographically and chemically similar but distinguishable by age, magnetic stratigraphy, and structural attitude (Kleibacker, 2001).

Individual flows are generally <10 m thick, range from massive to columnar jointed, and cannot be traced laterally for extended distances (McCutcheon, 2003). Lava flows from individual, submarine shield volcanoes coalesced to form oceanic islands. No volcanic edifices are preserved, but thick basaltic sections and a gravity anomaly located north of the Columbia

[1]GSA Data Repository item 2012170, locations of sample sites, chemical data for samples not listed in Table 1, and estimates of analytical uncertainty, is available at http://www.geosociety.org/pubs/ft2012.htm or by request to editing@geosociety.org.

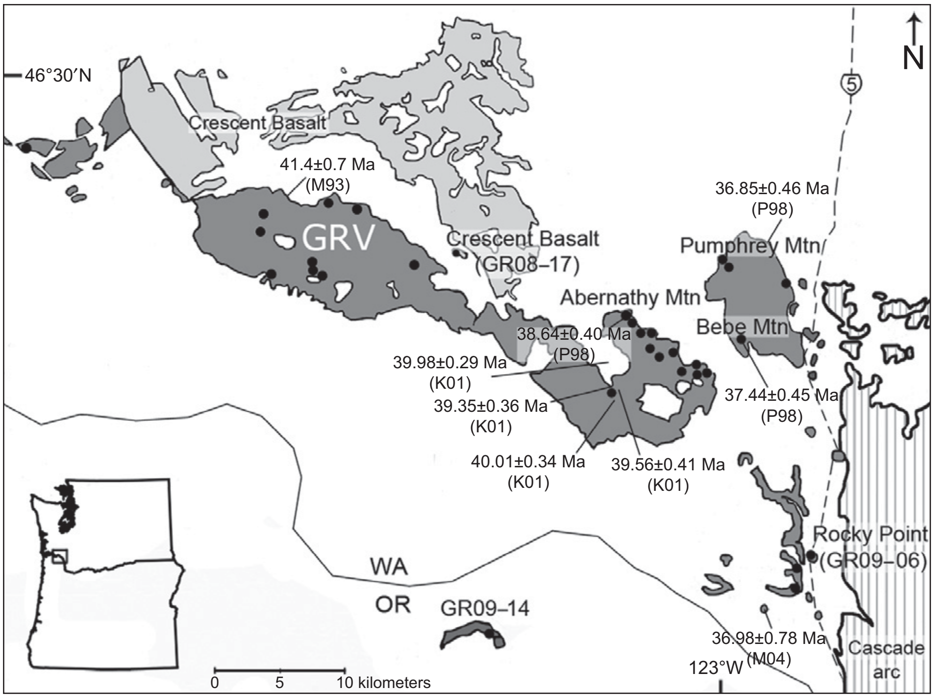

Figure 2. Simplified geologic map showing the outcrop area of the Grays River volcanics (GRV; in dark gray) and other nearby Tertiary volcanic rocks. Inset shows location of map area in southwest Washington–northwest Oregon. Interstate Highway I-5 is shown for reference. Geology was compiled from Walsh et al. (1987), Walker et al. (1991), and Eriksson (2002). Black dots indicate sample localities for this study. Ar-Ar ages, locations, and references for nine dated samples are indicated (M93—Moothart, 1993; P98—Payne, 1998; K01—Kleibacker, 2001; M04—McCutcheon, 2004). Note the general younger-to-the-NE age progression. The well that penetrated the greatest thickness of Grays River volcanics was located near sample locality GR09–14.

River and 32 km west of Longview suggest this may have been the location of an eruptive center (Finn et al., 1991). The thickest known section of the Grays River volcanics was encountered in an exploratory gas well at the southern edge of the outcrop area (Fig. 2), which penetrated >1700 m of basaltic lava flows, tuffs, and volcaniclastic rocks (Kenitz, 1997; Eriksson, 2002).

Interbedded with the Grays River lava flows, there are a variety of strata, including tuffs, fluvial, lacustrine, and marine sandstones, basaltic conglomerates, and coal lenses. To the east, subaerial Grays River volcanic flows interfinger with shallow-marine and deltaic arkosic sandstones and coal beds of the Cowlitz Formation, while to the west, submarine flows are interbedded with deep-marine facies of the McIntosh Formation and siltstones of the Tillamook Formation (Phillips et al., 1989). Grays River volcaniclastic rocks represent a series of debris flows and surge deposits and include flow breccias, conglomerates, sandstones, and siltstones that interfinger with sandstones and siltstones of the Cowlitz Formation (McCutcheon, 2003). The upper McIntosh and Cowlitz Formations are also intruded by thin (1–12 m) Grays River volcanic dikes, most of which trend southwest-northeast, although some secondary conjugate dikes oriented northwest-southeast are also present (Kleibacker, 2001).

METHODS

In total, 92 samples were collected from throughout the Grays River volcanic outcrop area (Fig. 2) as mapped by Walsh et al. (1987), Payne (1998), Kleibacker (2001), Eriksson (2002), and McCutcheon (2004). The best exposures were generally in road cuts and borrow pits. Fifty-five samples were fused with $LiBO_2$ for major- and trace-element analysis by inductively coupled plasma–atomic emission spectrometry (ICP-AES) at the University of Puget Sound; 20 of these samples were analyzed for additional trace elements by ICP mass spectrometry (MS) at Washington State University, and eight were analyzed for B and Be by ICP-AES at Puget Sound following an HF-mannitol digestion (Nakamura et al., 1992). Isotopic analyses of Sr, Nd, and Pb were performed on 12 samples at the University of Washington using a Nu instruments multicollector (MC) ICP-MS. Sr and Nd separations were performed following Nelson (1995); analytical procedures are described in Gaffney et al. (2007) for Nd and Brach-Papa et al. (2009) for Sr. The procedures for Pb separation and MC-ICP-MS analysis followed Harkins et al. (2008). Mineral analyses were performed by energy dispersive spectrometry (EDS) on a Hitachi 3400 scanning electron microscope (SEM) at the University of Puget Sound. Locations of sample sites, chemical data for samples not listed in Table 1, and estimates of analytical uncertainty are available as GSA Data Repository files (see footnote 1).

PETROGRAPHY

Grays River lavas are predominantly hiatal porphyritic basalts, typically with an aphanitic matrix. Phenocrysts account for 10%–15% of most samples and include plagioclase, olivine, augite, and ilmenite. Glomerophenocrysts of plagioclase ± clinopyroxene are also present and vary in size from 15 to 40 mm. The groundmass consists mostly of pilotaxitic plagioclase with lesser augite, orthopyroxene, ilmenite, and a greenish-brown phase that may represent altered glass. Secondary minerals, including zeolites, calcite, clays, and iddingsite, are ubiquitous and account for up to 15% of some Grays River volcanic samples.

Plagioclase

Plagioclase is the most abundant phenocryst phase (~70%) and typically also the largest, averaging ~16–18 mm in length, but reaching 3 cm in some instances. Compositions range from An_{74} to An_{39}, but variation within an individual zoned crystal is typically <5% An. No significant differences in An content between phenocrysts and groundmass were observed, although disequilibrium features, including sieve textures, are common in phenocrysts.

Olivine

Olivine phenocrysts ($Fo_{75–29}$) or their relics range from 2 to 20 mm in diameter and are present in ~30% of the sections. Intracrystalline zoning is minimal, and, in most cases, the original olivine has been largely replaced by iddingsite. Assuming K_d(ol/liq)/(Fe/Mg) = 0.31 (calculated for 3 kbar after Ulmer, 1989), olivines less magnesian than Fo_{60} are too Fe-rich to have crystallized from melts having compositions of the bulk rock. These Fe-rich olivines may be xenocrysts that originated within highly differentiated melt domains and were later mixed into more primitive magmas.

Pyroxene

Augite ($Wo_{48–37}En_{46–16}Fs_{36–11}$) is the second-most abundant phenocryst phase, occurring as euhedral-subhedral crystals ranging up to 24 mm in length and also in glomerocrysts with plagioclase. A few clinopyroxene phenocrysts are poikilitic with plagioclase inclusions. Clinopyroxene and orthopyroxene ($Wo_{11–2}En_{53–16}Fs_{79–45}$) are both present in the groundmass. No significant compositional differences are discernible between phenocryst and groundmass clinopyroxenes.

GEOCHEMISTRY

The majority of the 54 analyzed Grays River volcanic samples (Table 1; GSA Data Repository [see footnote 1]) are subalkaline to mildly alkaline (Fig. 3A), tholeiitic (Fig. 3B) basalts with limited SiO_2 variation (75% of samples have between 47 and 49 wt% SiO_2) (Fig. 3C). Greater variation is seen in Mg# (molar Mg/Mg + Fe_{Total}), which ranges from 0.59 to 0.32, and in the abundances of TiO_2, K_2O, P_2O_5, and incompatible trace elements, many of which display greater than fivefold variation in concentration (Figs. 4 and 5). With decreasing Mg#, Grays River volcanic samples show systematic increases in Na_2O, K_2O, P_2O_5, TiO_2, Zr, Y, and Sr (and other incompatible trace elements) and decreases in Ca and Sc (Figs. 4 and 5). It is notable, however, that significant variability also exists even among samples with similar Mg#s, as seen, for example, among samples with Mg# ~0.39, where K_2O ranges from 0.20 to 1.76 wt% and Zr ranges from 161 to 357 ppm (Figs. 4F and 5C).

Rare earth element (REE) patterns for all Grays River volcanics are similar (Fig. 6A), displaying moderate light (L) REE enrichment (La/Yb_N = 6–10), minimal heavy (H) REE fractionation (Dy/Yb_N < 2), and generally negligible Eu anomalies (Eu/Eu* = 0.84–1.08). On a spidergram (Fig. 6B), most samples have smooth convex profiles typical of OIB, in which Nb and Ta show the greatest enrichments. Two samples have profiles that differ from the rest: GR09–20, a basaltic andesite, shows depletions in Sr, P, and Ti, and GR09–04 has anomalously low abundances of all incompatible elements. This sample is also the only one with a LREE-depleted REE pattern (La/Sm_N < 1).

The B/Be ratios, which increase if slab-derived fluids are involved, are extremely low, with all but one value falling in the range 0.7–2.5 (Table 1; GSA Data Repository [see footnote 1]). The only sample with a higher value (6.1) is GR09–14, which is among the southernmost samples and thus is probably also older. Variation in B/Be is largely controlled by variation in B content (5.5–50.2 ppm), as Be concentrations are more uniform (4.1–8.4 ppm).

TABLE 1. REPRESENTATIVE WHOLE-ROCK CHEMICAL ANALYSES OF THE GRAYS RIVER VOLCANICS

Sample	GR08–1	GR08–19	GR08–148	GR09–03	GR09–04	GR09–07	GR09–10	GR09–11	GR09–14	GR09–16	GR09–20	GR09–22
Major oxide (wt%)												
SiO_2	50.23	48.35	48.79	47.01	45.93	47.83	46.96	47.85	48.61	48.00	53.48	45.66
TiO_2	3.44	2.94	3.85	3.15	3.24	3.62	2.83	3.75	3.72	3.46	2.11	3.11
Al_2O_3	14.70	14.86	14.41	14.36	15.43	15.31	11.69	14.30	14.92	14.63	14.61	15.40
Fe_2O_{3T}	13.90	13.54	14.12	14.31	15.73	13.50	13.33	13.75	13.92	14.12	11.29	14.30
MgO	3.68	5.56	4.56	6.02	5.77	4.62	9.53	5.29	4.04	4.93	4.07	6.00
MnO	0.27	0.18	0.19	0.21	0.21	0.17	0.15	0.16	0.18	0.17	0.16	0.19
CaO	8.34	10.90	9.25	11.73	10.15	10.82	12.24	10.45	9.76	10.34	8.35	11.20
Na_2O	3.63	2.73	3.31	2.55	2.72	3.00	2.08	2.99	3.39	2.92	3.94	2.98
K_2O	1.15	0.55	0.78	0.27	0.56	0.71	0.82	0.89	0.96	0.79	1.69	0.73
P_2O_5	0.64	0.39	0.75	0.40	0.24	0.43	0.37	0.57	0.50	0.63	0.30	0.43
LOI				3.76	3.54	3.09	3.20	2.04	2.25	3.40	1.50	7.90
ORIG TOTAL				100.57	97.28	100.03	101.26	96.64	99.47	100.92	101.75	97.94
Mg#	0.34	0.45	0.39	0.45	0.42	0.40	0.59	0.43	0.37	0.41	0.42	0.45
Trace element (ppm)												
Zr	342	197	282	212	165	272	208	251	308	278	447	248
Sr	513	364	462	422	365	537	366	480	478	439	372	496
Y	47	32	44	31	38	33	27	38	39	43	46	33
Sc	23	30	25	29	32	25	38	29	29	27	25	28
Cr	8	49										
Ba	232	182	273	156	66	266	176	211	257	190	401	254
Th	3.39	2.93	4.26	2.74	0.55	3.77	2.82	3.15	3.85	3.38	6.73	3.37
Nb	36.95	34.71	46.05	33.85	11.60	44.55	34.15	39.75	45.76	41.82	64.48	39.45
Hf	6.06	5.65	7.36	5.62	4.81	6.83	5.37	6.31	7.64	6.93	10.71	6.08
Ta	2.44	2.28	4.55	3.83	0.75	4.39	3.53	6.47	3.00	5.48	5.54	2.53
U	0.97	0.83	1.17	0.79	0.18	1.08	0.78	0.89	1.14	1.00	1.90	0.92
Pb	2.7	3.04	2.53	1.77	10.35	2.30	1.56	1.66	1.98	2.03	3.33	2.16
Rb	17.7	9.3	12.94	2.19	1.59	20.28	9.47	5.12	12.04	17.12	38.75	8.71
Cs	0.18	0.21	0.23	0.01	0.04	0.33	0.26	0.05	0.17	0.19	0.26	0.07
La	30.42	28.01	40.67	28.07	9.73	36.36	27.94	34.13	37.57	35.94	52.38	31.56
Ce	66.23	61.27	89.56	62.64	27.10	79.05	60.61	76.88	82.87	80.58	107.32	68.75
Pr	8.58	8.01	11.79	8.22	4.46	10.16	7.88	10.20	10.86	10.68	13.07	8.90
Nd	36.34	34.05	50.07	35.24	23.09	42.60	33.39	44.17	45.38	46.16	51.11	36.94
Sm	8.46	7.97	11.64	8.22	7.09	9.64	7.62	10.34	10.43	10.72	10.96	8.20
Eu	2.77	2.64	3.70	2.78	2.51	3.07	2.50	3.55	3.40	3.45	2.94	2.69
Gd	8.39	7.94	11.46	8.10	8.09	9.00	7.28	10.07	9.99	10.73	10.12	7.96
Tb	1.31	1.24	1.76	1.26	1.37	1.38	1.11	1.53	1.57	1.65	1.63	1.25
Dy	7.49	7.05	9.91	7.19	8.36	7.74	6.18	8.55	8.88	9.41	9.47	7.06
Ho	1.44	1.34	1.87	1.35	1.64	1.41	1.13	1.57	1.68	1.78	1.82	1.34
Er	3.62	3.31	4.60	3.26	4.12	3.33	2.71	3.89	4.09	4.30	4.72	3.32
Tm	0.49	0.44	0.62	0.43	0.58	0.45	0.37	0.50	0.55	0.58	0.65	0.46
Yb	2.84	2.55	3.61	2.55	3.44	2.54	2.04	2.92	3.18	3.34	3.94	2.67
Lu	0.43	0.38	0.54	0.37	0.52	0.37	0.30	0.42	0.47	0.52	0.60	0.40
B							6.91	5.57	49.48			15.85
Be							6.57	7.50	8.20			6.53

Note: Major oxides are normalized to 100% anhydrous. Total Fe is expressed as Fe_2O_3. LOI—loss on ignition.

Geological Society of America Bulletin, published online on 3 May 2012 as doi:10.1130/B30576.1

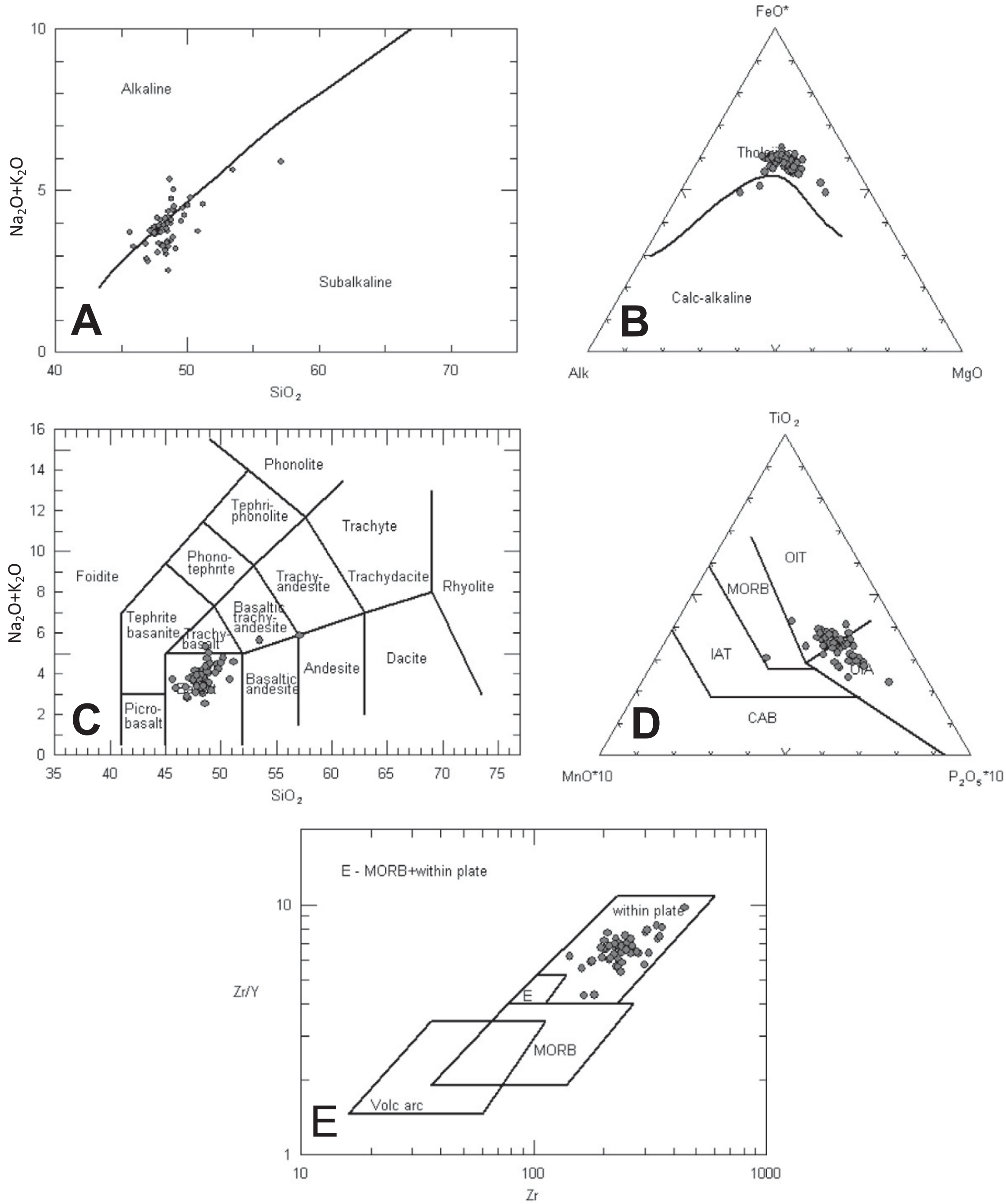

Figure 3. Geochemical classification diagrams for the Grays River volcanics. (A) Total alkalis (wt%) versus silica (wt%) plot (Irvine and Baragar, 1971) showing the Grays River volcanics are subalkaline to mildly alkaline. (B) AFM diagram (Irvine and Baragar, 1971) illustrating the tholeiitic character of the Grays River volcanics. (C) Classification diagram of Le Bas et al. (1986) showing the Grays River volcanics are almost exclusively basalts. (D–E) Discrimination plots (Mullen, 1983; Pearce and Norry, 1979) showing the ocean-island basalt (OIB) affinity of the Grays River volcanics. CAB—calc-alkaline basalts; IAT—island arc tholeiites; MORB—mid-ocean ridge basalts; OIT—ocean island tholeiitic basalts.

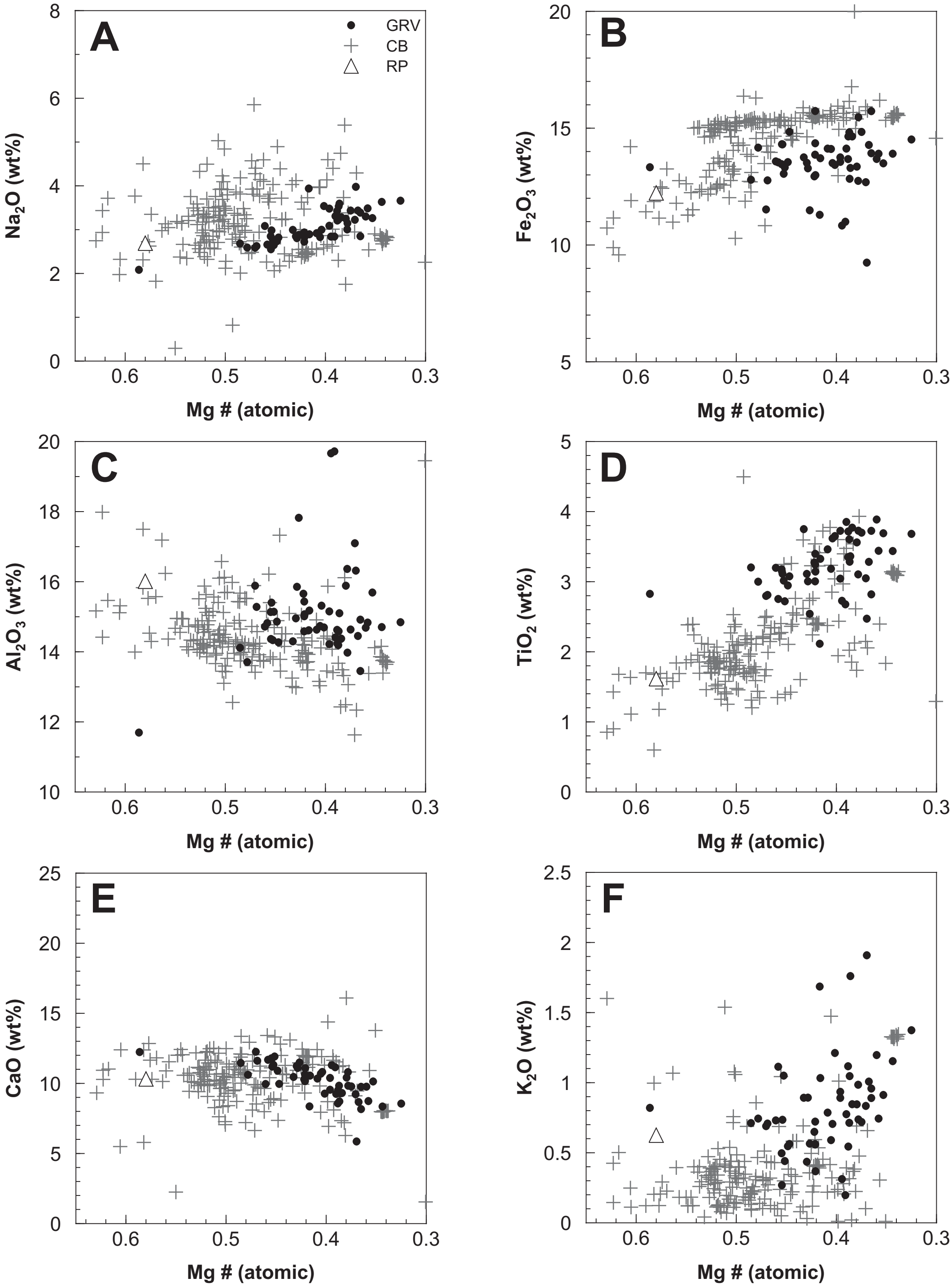

Figure 4. Major-element variation diagrams comparing the Grays River volcanics (GRV; black circles), Crescent Basalts (CB; gray crosses), and Rocky Point basaltic andesite (RP; open triangle).

Isotopic compositions of Grays River lavas (Table 2) show little variation for Sr ($^{87}Sr/^{86}Sr$ = 0.7034–0.7035) or Nd (ε_{Nd} = +5.0 to +5.5). The data form a tight cluster (Fig. 7A) that has considerably more radiogenic Sr and less radiogenic Nd than typical MORB (Hamelin and Allegre, 1985; Hegner and Tatsumoto, 1987; White et al., 1987; Debaille et al., 2006; Kellogg et al., 2007) and overlaps with values typical of the Cascade arc (Halliday et al., 1983; Bullen and Clynne, 1990; Bacon et al., 1994, 1997; Borg et al., 1997, 2000; Borg and Clynne, 1998; Grove et al., 2002; Leeman et al., 2004; Schmidt et al., 2008; Jicha et al., 2009). Measured $^{206}Pb/^{204}Pb$, $^{207}Pb/^{204}Pb$, and $^{208}Pb/^{204}Pb$ isotope ratios range from 19.359 to 19.525, 15.585 to 15.603, and 39.053 to 39.230, respectively (Table 2). Variations in $^{207}Pb/^{204}Pb$-$^{206}Pb/^{204}Pb$ (Fig. 7B) define a linear array on or slightly above the Northern Hemisphere reference line (NHRL) (Hart, 1984) and are within the field of basalts from the Oregon Coast Range (Pyle et al., 2009). The Grays River volcanics $^{206}Pb/^{204}Pb$ compositions are distinctly more radiogenic than Cascadia sediment (Church, 1976; Prytulak et al., 2006), Cascade lavas (Church and Tilton, 1973; Halliday et al., 1983; Bullen and Clynne, 1990;

Geological Society of America Bulletin, published online on 3 May 2012 as doi:10.1130/B30576.1

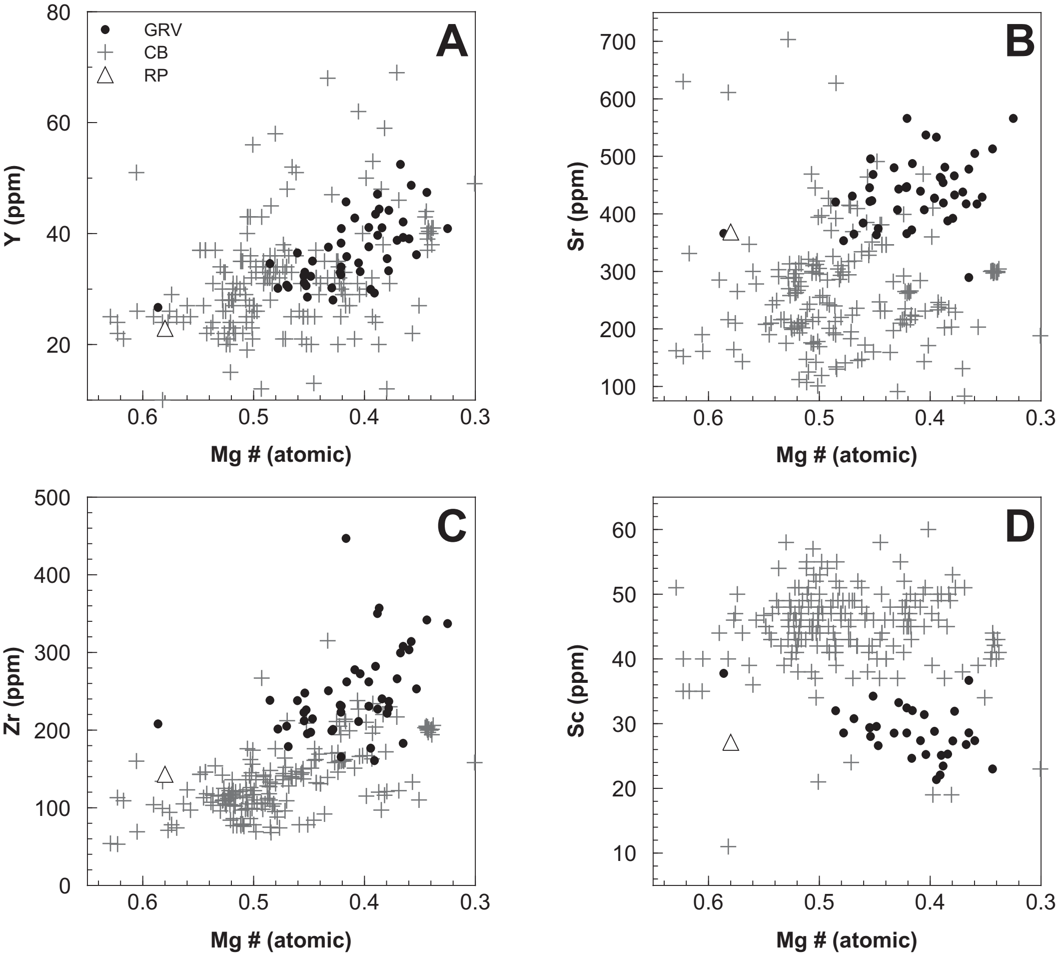

Figure 5. Trace-element variation diagrams comparing the Grays River volcanics (GRV; black circles), Crescent Basalts (CB; gray crosses), and Rocky Point basaltic andesite (RP; open triangle).

Leeman et al., 1990, 2004; Bacon et al., 1994, 1997; Borg et al., 1997, 2000, 2002; Borg and Clynne, 1998; Conrey et al., 2001; Grove et al., 2002; Schmidt et al., 2008; Jicha et al., 2009), and Juan de Fuca MORB (Hegner and Tatsumoto, 1987). A similar pattern is seen in $^{208}Pb/^{204}Pb$-$^{206}Pb/^{204}Pb$ (Fig. 7D), where the Grays River volcanics straddle the NHRL and have higher $^{208}Pb/^{204}Pb$ than Cascade arc rocks or Juan de Fuca MORB. Data for the Crescent Basalt and Rocky Point samples are markedly less radiogenic than the Grays River volcanics but also lie along the NHRL, the former plotting near other Crescent Basalt analyses (Pyle et al., 2009) and the latter falling within the Cascade arc field (Figs. 7C and 7D).

DISCUSSION

Grays River Volcanics Mantle Sources

The Grays River volcanics are broadly similar to ocean-island tholeiitic basalts (OIT) based on their trace-element patterns (Figs. 3D, 3E, 6B, and 8) and elevated levels of TiO_2, P_2O_5, and K_2O relative to MORB. These traits, together with the lack of HREE fractionation, indicate an asthenospheric mantle source with no residual garnet. An asthenospheric source is also implied by the absence of any evidence of a subduction component in the Grays River volcanics: Ta and Nb are not depleted relative to other incompatible trace elements (Fig. 6), $^{206}Pb/^{204}Pb$ ratios are high and preclude involvement of Cascadia sediment (Fig. 7B), and B/Be ratios are lower than in most Cascade arc lavas and comparable to ratios measured in OIB (Ryan et al., 1996a). For comparison, B/Be ratios of Quaternary Cascade lavas range from 2.4 to 7.8 (Smith and Leeman, 1987), and they in turn are at the low end of B/Be ratios (4.1–186) for arc rocks worldwide (Morris et al., 1990). Slab devolatilization generally leads to higher B/Be ratios in the forearc region than behind the volcanic front (Ryan et al., 1996b); low B/Be ratios in Grays River lavas argue against involvement of metasomatized mantle wedge in their generation. Other trace-element ratios indicative of contributions from the subducting slab are also low in the Grays River volcanics: Ba/La values (5.3–8.1) are in the range of normal (N) MORB (4–11) and well below arc values (>15) (Gill, 1981).

Indices of magma differentiation (e.g., Mg#, SiO_2 content) do not correlate with Sr-Nd-Pb isotopic variations, suggesting that crustal assimilation or contamination did not significantly influence magma compositions.

The Pb isotope data for Grays River volcanics are among the most radiogenic known from the Pacific Northwest and define linear arrays on Pb isotope diagrams that overlap ranges for other Coast Range basalts (Pyle et al., 2009) (Fig. 7D). Pyle et al. (2009) attributed the linear arrays defined by isotopic data for the Coast Range (Siletzia) basalts to source mixing between HIMU (High-μ isotopic reservoir) mantle and C mantle, the latter identified by Hanan and Graham (1996) as a deep OIB source region that is commonly sampled by mantle plumes. Isotopic traits of Grays River lavas closely match those of the C mantle component (Table 3; Figs. 7A–7D), suggesting they were dominantly derived from this deep plume source. Pyle et al. (2009) concluded that C is the main mantle source component in tholeiitic lavas throughout

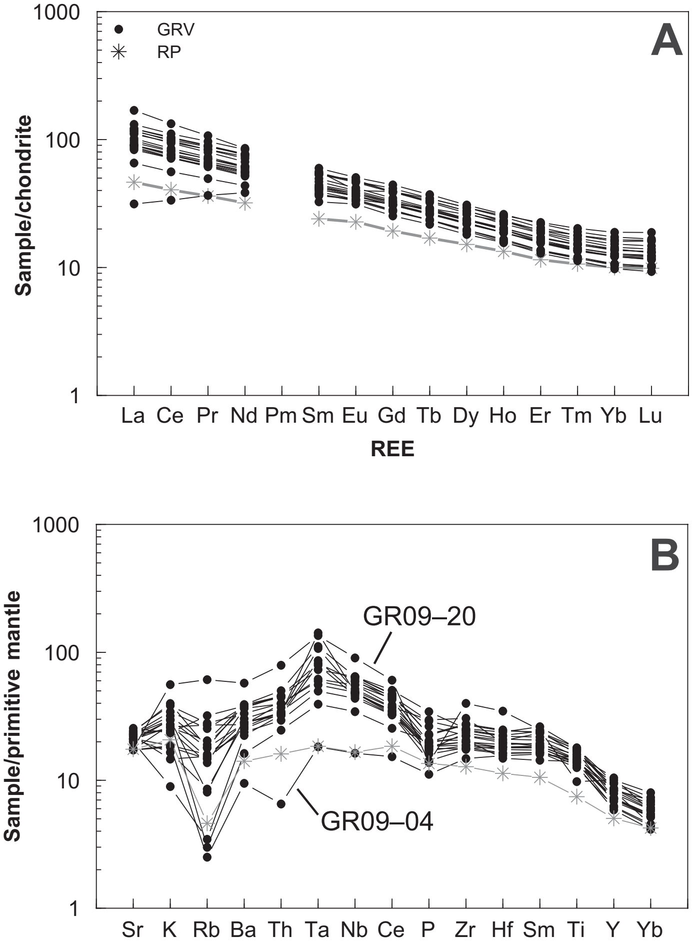

Figure 6. (A) Rare earth element (REE) plot for the Grays River volcanics (GRV) and Rocky Point (RP) basaltic andesite normalized to the chondrite values of Boynton (1984). Note that, with the exception of GR09–04, all samples have similar REE profiles with negligible Eu anomalies. (B) Spider diagram for the Grays River volcanics and Rocky Point basaltic andesite, normalized to the primitive mantle values of Sun and McDonough (1989). The concave profiles are characteristic of ocean-island basalt (OIB) magmas. All Ta data are from samples pulverized in an alumina shatterbox; the positive Ta anomalies seen in some samples are not attributable to contamination during sample preparation.

Siletzia and that involvement of the HIMU component diminishes north of Oregon. In Washington, isotopic analyses of the Crescent Basalts (Table 3) extend to less radiogenic Pb and Sr compositions, and higher ε_{Nd} values, than C mantle, defining linear trends on isotope (Figs. 7C and 7D) and trace-element diagrams (Fig. 8) that are consistent with mixing between C and a depleted mantle component. Although isotopic data for the Grays River volcanics show less variation and overlap entirely with C mantle (Table 3; Fig. 7), linear data arrays on both isotopic (Figs. 7C and 7D) and trace-element (Fig. 8) diagrams are indicative of source mixing. In summary, we conclude that Grays River lavas were derived from a mixed mantle source that was dominated by a C-like plume component but also contained lesser amounts of a depleted component.

Melt Segregation Depth and Magma Evolution

We estimated the depth of melt segregation by applying the thermobarometer of Lee et al. (2009) to the most primitive Grays River volcanics sample (GR09–10, Mg# = 0.59, 9.5 wt% MgO). Based on the exchange of Mg and Si between olivine plus orthopyroxene and melt, this thermobarometer is applicable to basaltic lavas that have undergone only olivine fractionation and have >8.5 wt% MgO (Lee et al., 2009). Assuming Fe^{+3}/Fe^{T} = 0.07 and Mg# = 0.90 for the mantle source, the calculated temperature and pressure are 1567 °C and 3.40 GPa. The latter is equivalent to ~100 km depth and indicates derivation from below the subducting slab. Parker et al. (2010) obtained similar temperatures (~1500–1700 °C) and depths (70–160 km) for primitive Coast Range basalts from Cascade Head and Yachats.

Low Mg#s (average = 41, with only one sample >50) and low Cr contents (average = 51 ppm) indicate most Grays River lavas have

TABLE 2. Sr-Nd-Pb ISOTOPE DATA FOR GRAYS RIVER, ROCKY POINT, AND CRESCENT FORMATION SAMPLES

Sample location	Sample	$^{143}Nd/^{144}Nd$	±2σ	ε_{Nd} (0)	±2σ	$^{87}Sr/^{86}Sr$	±2σ	[Rb]	[Sr]	$^{206}Pb/^{204}Pb$	$^{207}Pb/^{204}Pb$	$^{208}Pb/^{204}Pb$
Terra Firma Quarry	GR 09–01	0.512918	7	5.46	0.07	0.703443	8	5.4	445	19.456	15.592	39.141
Bebe Mtn	GR 09–10	0.512899	6	5.09	0.06	0.703530	9	9.5	366	19.525	15.597	39.230
Hwy 411	GR 09–11	0.512896	6	5.03	0.06	0.703446	7	5.1	480	19.504	15.590	39.200
9213 Quarry	GR 08–148	0.512898	5	5.06	0.05	0.703441	12	12.9	462	19.395	15.603	39.140
Fossil Creek 3	GR 08–04	0.512913	7	5.37	0.07	0.703472	11	10.1	414	19.359	15.588	39.053
SF800 Rd	GR 08–12	0.512910	8	5.31	0.08	0.703523	11	1.9	550	19.379	15.599	39.102
Hwy 30	GR 09–14	0.512910	6	5.30	0.06	0.703468	9	12.0	478	19.500	15.592	39.191
Germany Ck	GR 09–16	0.512907	6	5.24	0.06	0.703530	10	17.1	439	19.446	15.585	39.125
Pumphrey Mtn	GR 08–19	0.512911	5	5.32	0.05	0.703456	14	9.3	449	19.428	15.591	39.122
Germany Ck	GR 09–22	0.512899	7	5.08	0.07	0.703535	9	8.7	496	19.410	15.599	39.125
Crescent Basalt	GR 08–17	0.512965	5	6.38	0.05	0.703548	9		198	19.152	15.563	38.792
Rocky Point	GR 09–06	0.512986	8	6.79	0.08	0.703068	7	2.9	368	18.947	15.536	38.511

Note: Errors shown in table are within-run statistics and represent error in the last significant digits. The following is the external reproducibility at 2σ: Nd = +30 ppm; Sr= +30 ppm; Pb= +125, 150, and 200 ppm for $^{206}Pb/^{204}Pb$, $^{207}Pb/^{204}Pb$, and $^{208}Pb/^{204}Pb$, respectively. Pb isotope compositions are normalized to NIST-981 accepted values of $^{208}Pb/^{204}Pb$ = 36.721, $^{207}Pb/^{204}Pb$ = 15.491, $^{206}Pb/^{204}Pb$ = 16.937. Sr and Nd isotope compositions are normalized to $^{86}Sr/^{88}Sr$ = 0.1194 and $^{146}Nd/^{144}Nd$ = 0.7219, respectively. ε_{Nd} (0) is deviation from chondritic $^{143}Nd/^{144}Nd$ = 0.512638 in units of parts per 10^4. Rb and Sr concentrations (in ppm) are by inductively coupled plasma–mass spectrometry.

Geological Society of America Bulletin, published online on 3 May 2012 as doi:10.1130/B30576.1

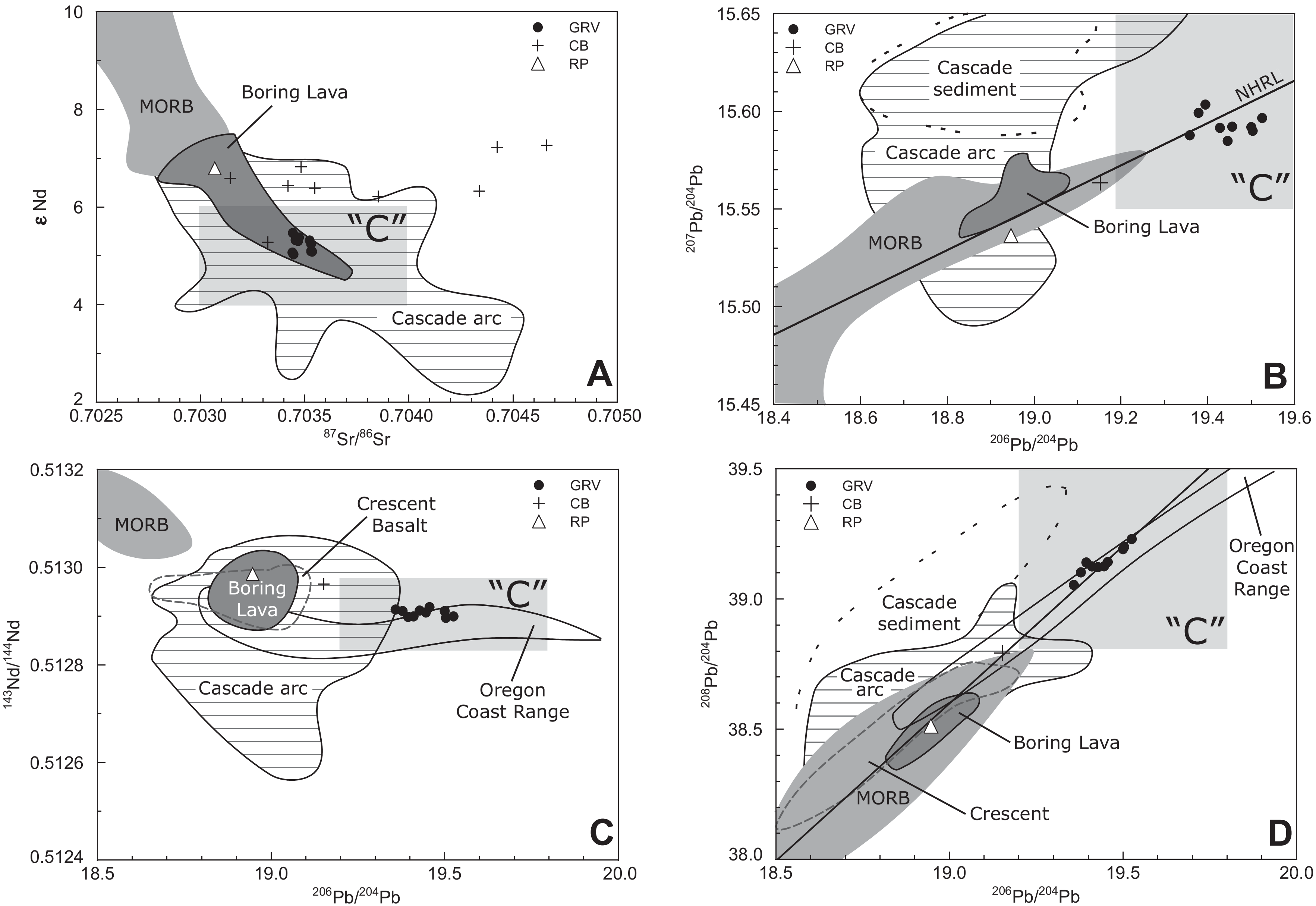

Figure 7. Sr-Nd-Pb isotope data of Grays River volcanics compared to data from other volcanic and sedimentary rocks in the Cascadia region. The gray box square labeled "C" in all plots delineates the composition of mantle component "C" as defined by Hanan and Graham (1996). Data sources for the other fields are as follows: Cascade arc (Church and Tilton, 1973; Church, 1976; Halliday et al., 1983; Bullen and Clynne, 1990; Leeman et al., 1990, 2004; Bacon et al., 1994, 1997; Borg et al., 1997, 2000, 2002; Borg and Clynne, 1998; Conrey et al., 2001; Grove et al., 2002; Jicha et al., 2009), mid-ocean-ridge basalt (MORB; Hamelin and Allegre, 1985; Hegner and Tatsumoto, 1987; White et al., 1987), Cascade sediments (Church, 1976; Prytulak et al., 2006), Boring Lava volcanic field (R. Conrey, personal commun., 2009), Crescent Basalts (Tepper et al., 2008; Pyle et al., 2009), and Oregon Coast Range (Pyle et al., 2009). GRV—Grays River volcanics; CB—Crescent Basalts; RP—Rocky Point basaltic andesite; NHRL—Northern Hemisphere reference line.

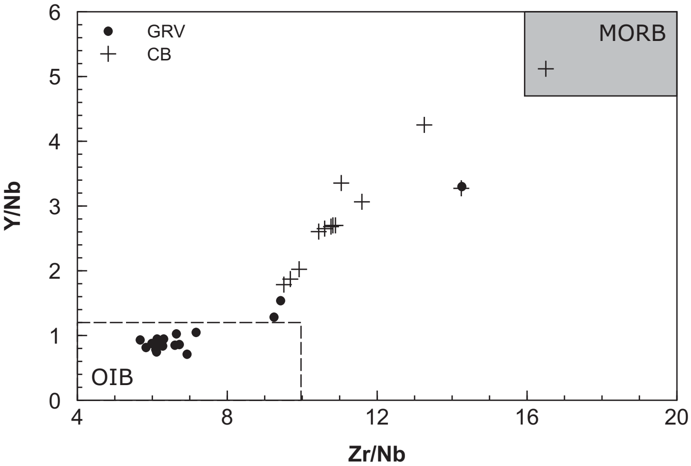

Figure 8. Incompatible trace-element ratios of the Grays River volcanics (GRV) and Crescent Basalts (CB) compared to typical values of mid-ocean-ridge basalt (MORB) and ocean-island basalt (OIB) (from LeRoux et al., 1983). The linear data arrays suggest that both units were derived from mixed mantle sources, but the Grays River volcanics were dominated by an OIB-type source, whereas the Crescent Basalts had a larger depleted mantle component. See text for further discussion.

undergone significant differentiation. Elemental trends that accompany differentiation, specifically the increase in Sr (Fig. 5B), decrease in Sc (Fig. 5D), lack of SiO_2 enrichment (>90% of samples have between 46 and 51 wt% SiO_2), and absence of appreciable Eu anomalies (Fig. 6A), indicate that differentiation was dominated by removal of clinopyroxene, with minimal plagioclase and olivine fractionation. This assemblage implies crystallization at lower- or subcrustal depths (>30 km; Bender et al., 1978). The maximum depth of differentiation is constrained to ≤80 km based on the unfractionated REE patterns, which preclude garnet fractionation (Wyllie, 1981; Takahashi et al., 1993; Hirschmann and Stolper, 1996).

The low Mg#s of the more evolved Grays River samples indicate that the amount of crystallization was high. This conclusion is supported by a greater than fourfold variation in the levels of several incompatible major and trace elements, which if due solely to crystal fractionation would require >75% crystallization. This is greater than the 43–50 wt% clinopyroxene fractionation necessary to produce a typical Grays River lava (Mg# = 41) from a primary magma (Mg# = 66), calculated assuming that K_d(ol/liq)/(Fe/Mg) = 0.22–0.28 (Nielsen et al., 1988). Modest removal of olivine and/or plagioclase may also have occurred, but that does not change the basic conclusion, also required by the isotopic data, that some of the incompatible element variation likely reflects source heterogeneity, particularly where the variation exists among samples with similar Mg#s (Figs. 5A, 5B, and 5C).

Comparison with Other Coast Range Volcanic Units

Crescent Basalts (CB)

Basalts of the ca. 54–48 Ma Crescent Formation represent an earlier and more voluminous episode of Coast Range volcanism that predated establishment of the modern Cascade arc. Comparison of Grays River volcanics analyses with a Crescent Basalt data set of 205 major- and trace-element analyses (K. Clark, personal commun., 2009) and eight Sr-Nd isotopic analyses (Tepper et al., 2008) reveals that the Crescent Basalts are more compositionally diverse (Mg# = 63–34; Fig. 4) but on average less differentiated (avg. Mg# = 0.46 vs. 0.41), less depleted in Sc (Fig. 5D), and less enriched in incompatible elements, including TiO_2, K_2O, P_2O_5, Sr, and Zr (Figs. 4 and 5). REE patterns for Crescent Basalts are less LREE enriched (avg. La/Yb_N = 2.7 vs. 7.4 for Grays River volcanics). Most Crescent Basalts samples have distinctly higher ε_{Nd} (+6.2 to +7.3) than the Grays River volcanics (+5.0 to + 5.5), although one Crescent Basalt sample overlaps the Grays River volcanics data (Fig. 7A). The large scatter in $^{87}Sr/^{86}Sr$ of the Crescent Basalts lavas (Fig. 7A) is most likely due to seawater interaction, which apparently did not affect the Grays River volcanic samples. Pb isotope compositions of Crescent Basalts are less radiogenic than the Grays River volcanics (Figs. 7B, 7C, and 7D). Taken together, these chemical and isotopic differences indicate that the Grays River volcanics were derived from a less depleted mantle source than the Crescent Basalts. It is also possible that smaller degrees of melting may have contributed to the higher incompatible element contents of the Grays River volcanics. However, it is important to note that within the Crescent Basalt data set, there are some samples with elevated incompatible element contents (Figs. 4 and 5) or ε_{Nd} values (Fig. 7A) that overlap with Grays River lavas. This suggests that domains of more enriched Grays River volcanics source mantle were present within the Crescent Basalts source, but not extensively involved during that earlier melting episode. Following melt generation, it appears that Crescent Basalt magmas on average differentiated less, and at shallower depth (less pyroxene removal, more feldspar removal), than Grays River magmas. This is indicated by the generally higher Sc, Fe_2O_3, and Al_2O_3 contents, and generally lower Sr contents of the Crescent Basalts (Figs. 4 and 5).

Tillamook Volcanics (TV)

Centered ~100 km to the south of the Grays River volcanics, the 46–40 Ma Tillamook volcanics are slightly older than the Grays River volcanics but of similar petrological character (Niem et al., 1992b; Kenitz, 1997). Data on Tillamook lavas, which are dominantly basalts but extend to dacites, are limited to major-element analyses (Rarey, 1985; Mumford, 1988; Safley, 1989). These show substantial overlap between the Tillamook volcanics and Grays River volcanics for all major oxides including

TABLE 3. COMPARISON OF ISOTOPIC COMPOSITIONS OF GRAYS RIVER LAVAS, CRESCENT BASALTS, SILETZIA LAVAS, AND MANTLE COMPONENT C

	Grays River*	"C" component†	Crescent*§#	Siletzia#
$^{206}Pb/^{204}Pb$	19.36–19.53	19.2–19.8	18.5–19.2	18.56–19.94
$^{207}Pb/^{204}Pb$	15.58–15.60	15.55–15.65	15.56	15.49–15.68
$^{208}Pb/^{204}Pb$	39.05–39.23	38.8–39.6	38.1–38.7	38.13–39.53
$^{87}Sr/^{86}Sr$	0.7034–0.7035	0.703–0.704	0.7031–0.7047	0.7031–0.7037
ε_{Nd}	+5.0 to +5.5	+4 to +6	+5.3 to +7.3	+5.0 to +7.7

*This study.
†Hanan and Graham (1996).
§Tepper, unpub. data.
#Pyle et al. (2009).

Geological Society of America Bulletin, published online on 3 May 2012 as doi:10.1130/B30576.1

TiO_2 (Tillamook avg. = 3.03 wt%) and K_2O (Tillamook avg. = 1.16 wt%), but establishing any links between the Tillamook volcanics and Grays River volcanics will require additional trace-element and isotopic data.

Rocky Point (RP)

The Rocky Point volcanic center at the eastern edge of the Grays River volcanics consists of basalt flows, hyaloclastites, and scoriaceous breccias that are petrographically similar to Grays River basalts. The sample we examined contained phenocrysts of plagioclase (An_{80-33}), olivine (Fo_{73-48}), and clinopyroxene ($Wo_{30}En_{40}Fs_{30}$) in a groundmass of those same minerals plus orthopyroxene, ilmenite, and alteration phases. While Rocky Point lavas interfinger with Grays River volcanic flows, our chemical and isotopic data confirm the suggestion of McCutcheon (2003) that the two units are distinct. Compared to Grays River volcanic basalts, the Rocky Point sample has a higher Mg# (0.58), lower incompatible element contents (e.g., TiO_2, Zr, Y) (Figs. 4 and 5), and less LREE enrichment (Fig. 6A). It also displays arc-like chemical traits not seen in the Grays River volcanics, including elevated Ba/Nb and B/Be, and Sr-Nd-Pb isotopic compositions that overlap with those of modern Cascade arc rocks (Fig. 7). We interpret Rocky Point as an early Cascade arc volcanic center and infer that these magmas originated from a lithospheric (mantle wedge) source that was both more depleted than the Grays River volcanics source and also more affected by subduction-related metasomatism.

Boring Lavas (BL)

The 2.6–0.2 Ma Boring Lava volcanic field is located ~120 km southeast of the Grays River area and represents the youngest episode of Cascadia forearc volcanism. These compositionally diverse mafic to intermediate lavas erupted from >80 individual volcanic centers in and around the Portland Basin. They display a temporal trend from early low-K tholeiites and OIB that lack subduction traits to later calc-alkaline basalts and high-K calc-alkaline basalts (Conrey, 2009). Comparison of our Grays River volcanics data with analyses of 400 Boring Lava basalts (R. Conrey, personal commun., 2009) reveals that the Boring Lava are consistently more primitive (average Mg# > 55, average Cr > 200 ppm), higher in Ba/Nb (avg. > 15 vs. <6 for the Grays River volcanics), and isotopically different in Pb ($^{206}Pb/^{204}Pb < 19.1$ vs. >19.3 for Grays River volcanics), although not in Sr or Nd (Fig. 7A). Of the four Boring Lava basalt types, the OIB most closely resembles the Grays River volcanics, overlapping in K_2O and P_2O_5, but the Boring Lava OIB are notably lower in TiO_2 (avg. 1.7 vs. 3.2 wt%) and higher in Sr (avg. 605 vs. 440 ppm). No isotopic data are available for the OIB type of Boring Lava. Taken together, these data indicate three main factors are responsible for differences between the Grays River volcanics and Boring Lava: (1) The Grays River volcanics originated from a more enriched (plume) asthenospheric source, (2) the Grays River volcanics interacted less with the subducting slab and/or metasomatized mantle wedge, and (3) the Grays River volcanics underwent more extensive differentiation.

Tectonic Setting

Some attributes of the Grays River volcanics are indicative of a mantle plume or hotspot setting, while others are better explained by a rift or slab window setting. Strong evidence for a mantle plume tectonic setting comes from the radiogenic Pb isotope data, which closely match the inferred composition of the common plume component known as C (Hanan and Graham, 1996). The Pb isotope data also document a link between the Grays River volcanics and earlier Siletzia basalts, for which a hotspot origin is further indicated by high $^3He/^4He$ ratios and by the very large volume of material (~2.6×10^6 km^3) erupted within a short (~6 m.y.) time span (Pyle et al., 2009).

While the Pb isotope data and link to Siletzia magmatism imply a mantle plume setting, temporal and spatial data for the Grays River volcanics are more consistent with a slab window setting. Evidence indicative of a slab window includes the following: (1) The northward-younging age progression of the Tillamook and Grays River volcanics is consistent with plate motion reconstructions (Babcock et al., 1992) that indicate the Farallon plate was moving NE relative to North America at ~70 km/m.y. (2) Plate reconstructions indicate North America was moving westward at 20–30 km/m.y. relative to a fixed hotspot reference frame during the late Eocene (Babcock et al., 1992). Volcanism associated with a hotspot should thus display an eastward-younging age progression, one nearly perpendicular to the observed Tillamook–Grays River volcanics progression. (3) Plate reconstructions consistently indicate that a spreading ridge was located off of, and was subducting beneath, the Oregon-Washington coast during the Eocene (Engebretson et al., 1985; Haeussler et al., 2003; Madsen et al., 2006). (4) Outcrops of 47–43 Ma adakites on the Olympic Peninsula (Tepper et al., 2004) and 51–35 Ma forearc intrusions on Vancouver Island (Madsen et al., 2006) provide on-land evidence of multiple northward-migrating slab windows in the Cascadia forearc during the Eocene. (5) There is no evidence for interaction with subduction-modified material in Grays River lavas. A slab window provides a means for asthenospheric melts, which are calculated to have segregated at ~100 km depth, to reach the surface without interacting with the subducting slab or the metasomatized mantle wedge. (6) Northward movement of the Farallon plate relative to a fixed hotspot (Babcock et al., 1992) would result in continuous delivery of new slab into the ascent path of the plume. This would present a persistent thermal obstacle to the plume, and others have concluded that it is unlikely a plume could burn through cold subducting lithosphere and produce a volcanic chain parallel to the plate boundary (Morris and Hart, 1983; Geist and Richards, 1993).

Integrating these constraints, we propose that the Grays River volcanics formed in a slab window setting, but one in which the subducting ridge was influenced by a nearby mantle plume or plume head (Fig. 9). Johnston and Thorkelson (2000) located the Yellowstone plume beneath southern or central Oregon during the Eocene, and Pyle et al. (2009) argued that this plume was responsible for the voluminous Coast Range volcanism that began in southern Oregon at ca. 56 Ma. Farther north, mixing between plume source (C component) mantle and depleted mantle produced the mid-Eocene Crescent Basalts and late Eocene Grays River volcanics. This mixing is reflected in the diversity of MORB and OIB signatures seen in Crescent lavas (Babcock et al., 1992) as well as linear arrays on chemical and isotopic plots for Grays River volcanics (Figs. 7 and 8). While proximity to a hotspot exerted a dominant influence on Grays River magma composition, the northward-younging pattern of magmatism was controlled by subduction of the northward-migrating Kula-Farallon Ridge, which produced a series of slab windows beneath Washington and British Columbia. Tomographic imaging of Pacific Northwest mantle suggests fragmentation of the subducted Juan de Fuca slab and the existence of slab windows that may have allowed upwelling asthenosphere during formation of Siletzia (Obrebski et al., 2010). Regional geochemical trends also provide support for upwelling asthenosphere passing through slab windows and displacing hydrated mantle wedge (Thorkelson et al., 2011).

Comparisons with Mafic Magmas in Other Slab Window Settings

Mafic lavas with OIB affinities have been described from other slab window settings, including Patagonia (Gorring and Kay, 2001), Costa Rica (Abratis and Wörner, 2001), Baja California (Benoit et al., 2002), and the Antarctica

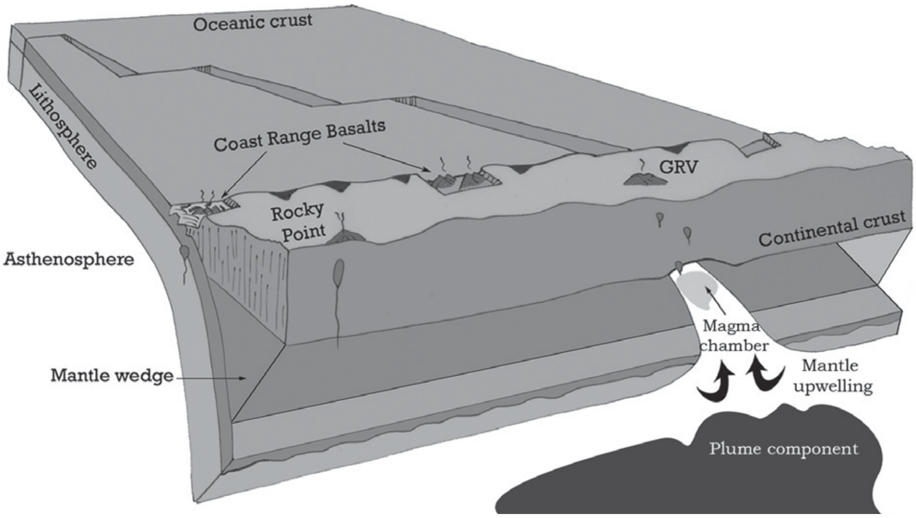

Figure 9. Schematic illustration of the tectonic setting of Eocene magmatism in the Cascadia forearc. The Grays River volcanics (GRV) formed above a slab window that allowed asthenospheric mantle containing a plume component to ascend through the subducting slab and mantle wedge. The Crescent Basalts erupted in marginal basins, while Rocky Point lavas were derived from the mantle wedge and are representative of more typical Cascade arc magmatism. See text for further discussion.

Peninsula (Hole et al., 1993). In all of these cases, magmatism is attributed to decompression melting of asthenospheric mantle that ascended into the gap formed by an opening slab window. Although the cause of magmatism was the same, these localities display chemical and isotopic diversity caused by variations in: (1) asthenosphere composition, (2) degree of melting and/or depth of melt separation, and (3) extent of interaction with the mantle wedge, subducting slab, and/or crust. Differences in asthenosphere composition are most clearly seen in Pb isotope data, with $^{206}Pb/^{204}Pb$ ranging from 18.3 to 18.8 in Patagonia (Gorring and Kay, 2001) to 19.1–19.3 in Costa Rica (Abratis and Wörner, 2001). Costa Rica is the closest analog for the Grays River volcanics ($^{206}Pb/^{204}Pb$ = 19.36–19.53); radiogenic Pb compositions there are attributed to decompression melting of upwelling asthenosphere that contained a plume component related to the Galapagos hotspot (Abratis and Wörner, 2001).

Fractionated HREE patterns indicate that slab window basalts from Patagonia and the Antarctic Peninsula separated from their source regions within the garnet stability field at depths >70 km (Hole et al., 1993; Gorring and Kay, 2001). At other localities, including the Grays River volcanics, the mafic rocks show no REE evidence of a source with residual garnet. However, the close spatial and temporal association with adakites (which require garnet in the source) in Costa Rica (Abratis and Wörner, 2001) and Baja California (Benoit et al., 2002), and the results of Mg-Si thermobarometry for the Grays River volcanics (discussed herein) suggest that the lack of a garnet signature in these cases may reflect a higher degree of melting and consumption of garnet rather than a shallower depth of segregation.

In most slab window settings, the mafic lavas show evidence of contamination by material with an arc signature, potentially subduction-modified mantle wedge or the crust. Such contamination is most commonly indicated by trace-element data, including elevated Ba/La (>10) and low Ce/Pb (<20) and Nb/U (<35) ratios (Abratis and Wörner, 2001; Gorring and Kay, 2001). By all of these measures, the Grays River volcanics are less contaminated than their counterparts from other arcs, with average ratios of Ce/Pb (32.5), Nb/U (42), and Ba/La (6.8) that are in the range for OIB and/or MORB (Gorring and Kay, 2001). One factor that probably contributed to the lack of contamination was a thinner lithosphere beneath the Grays River volcanics as a consequence of the forearc setting. In contrast, OIB-like lavas from Patagonia, Costa Rica, and Antarctica mainly erupted within or behind the arc and thus would have ascended through a thicker section of lithosphere.

SUMMARY AND CONCLUSIONS

The Grays River volcanics are the product of two major tectonic events that affected Cascadia during the Eocene: (1) subduction of one or more spreading ridges, including the Kula-Farallon, and (2) appearance of a mantle plume, probably the Yellowstone hotspot. Intersection of one or more spreading ridges with the Cascadia margin during the Eocene produced a series of northward-migrating slab windows (Madsen et al., 2006) that explain the northward-younging trend of the Grays River volcanics as well as the absence of any subduction signature in the rocks. Mantle beneath the Kula-Farallon Ridge at this time was influenced by a nearby mantle plume, possibly the Yellowstone hotspot, and this is reflected in the OIB traits of Grays River lavas, most notably their radiogenic Pb isotope ratios. These isotopic data establish that the Grays River volcanics share a common mantle source with earlier, more voluminous Coast Range basalts, including the Crescent Formation in Washington. It is notable that aside from these Coast Range lavas, rocks with $^{206}Pb/^{204}Pb$ > 19.1 are virtually unknown from the Cascadia region, the exception being Pleistocene basalts from the Simcoe field in southern Washington (Church and Tilton, 1973; Bacon et al., 1997; Leeman et al., 1990, 2004). This implies that the Coast Range basalts originated from a mantle source that was not present, or at least not sampled, during earlier or later igneous episodes in the region.

Although the Grays River volcanics share some plume source characteristics with the Crescent Formation, they differ in being generally more enriched (e.g., higher incompatible element abundances, lower ε_{Nd}, more radiogenic Pb isotope compositions) and less voluminous. Many of the same differences are seen elsewhere in the Coast Ranges when comparing early Eocene versus late Eocene volcanic units. Two factors may account for decreased involvement of a depleted mantle component and greater involvement of the plume component in the younger rocks. First, by the late Eocene, there had been more time for plume material to migrate northward, which would enhance its role in magma generation. Second, the younger units were emplaced above a slab window rather than on the ocean floor or in marginal rift basins. The slab window, as it grew wider, would have facilitated ascent of deeper mantle material, leading to a broader region of upwelling asthenosphere and less mixing with depleted lithospheric mantle.

In Cascadia, it appears that transient tectonic events, specifically, the arrival of a mantle plume and passage of a slab window, were responsible for much of the geochemical and isotopic variation in forearc magmatism over the 50 m.y. interval represented by the Crescent Basalts, Grays River volcanics, and Boring Lavas. These tectonic events influenced the compositions of asthenospheric melts and the extent to which ascending magmas interacted with the mantle wedge. Only the Boring Lavas, which were not associated with a slab window, show evidence of interaction with the mantle wedge. We conclude that because most Cascadia forearc magmas did not sample the supraslab mantle wedge, they do not record its temporal evolution. However, these magmas do reveal a unique plume signature that characterizes asthenosphere-derived magmas generated in this region during the Eocene. Identification of this fingerprint provides a powerful tool for further investigating the role of slab window magmatism throughout the Pacific Northwest.

ACKNOWLEDGMENTS

We thank Rick Conrey, Doug Pyle, and Ken Clark for sharing unpublished data, Lucy Kruesel and Mike Valentine for field assistance and support, and the Hancock Timber Group and Weyerhaeuser Corporation for permission to sample on their lands. Partial funding for this project was provided by a University of Puget Sound McCormick Fellowship to Chan. The Pb isotope analyses were funded by Paul Hammond and Al Niem. We also acknowledge data provided by the Fall 2008 Igneous Petrology class students at the University of Puget Sound (Tacoma, WA); this research began as their class project. The manuscript benefited from thoughtful reviews by Don Parker and Derek Thorkelson.

REFERENCES CITED

Abratis, M., and Wörner, G., 2001, Ridge collision, slab-window formation, and the flux of Pacific asthenosphere into the Caribbean realm: Geology, v. 29, p. 127–130, doi:10.1130/0091-7613(2001)029<0127:RCSWFA>2.0.CO;2.

Armentrout, J.M., 1987, Cenozoic stratigraphy, unconformity-bounded sequences, and tectonic history of southwestern Washington, *in* Schuster, J.E., ed., Selected Papers on the Geology of Washington: Washington Department of Natural Resources, Division of Geology and Earth Resources Bulletin, v. 77, p. 291–320.

Babcock, R.S., Burmester, R.F., Engebretson, D.C., Warnock, A., and Clark, K.P., 1992, A rifted margin origin for the Crescent Basalts and related rocks in the Northern Coast Range volcanic province, Washington and British Columbia: Journal of Geophysical Research, v. 97, p. 6799–6821, doi:10.1029/91JB02926.

Bacon, C.R., Gunn, S.H., Lanphere, M.A., and Wooden, J.L., 1994, Multiple isotopic components in Quaternary volcanic rocks of the Cascades arc near Crater Lake, Oregon: Journal of Petrology, v. 35, p. 1521–1556.

Bacon, C.R., Bruggman, P.E., Christiansen, R.L., Clynne, M.A., Donnelly-Nolan, J.M., and Hildreth, W., 1997, Primitive magmas at five Cascade volcanic fields: Melts from hot, heterogeneous sub-arc mantle: Canadian Mineralogist, v. 35, p. 397–423.

Beck, M.E., and Burr, C.D., 1979, Paleomagnetism and tectonic significance of the Goble volcanic series, southwestern Washington: Geology, v. 7, p. 175–179, doi:10.1130/0091-7613(1979)7<175:PATSOT>2.0.CO;2.

Bender, J.F., Hodges, F.N., and Bence, A.E., 1978, Petrogenesis of basalts from the project FAMOUS area: Experimental study from 0 to 15 kbars: Earth and Planetary Science Letters, v. 41, p. 277–302, doi:10.1016/0012-821X(78)90184-X.

Benoit, M., Aguillon-Robles, A., Calmus, T., Maury, R.C., Bellon, H., Cotton, J., Bourgois, J., and Michaud, F., 2002, Geochemical diversity of late Miocene volcanism in southern Baja California, Mexico: Implication of mantle and crustal sources during the opening of an asthenospheric window: The Journal of Geology, v. 110, p. 627–648, doi:10.1086/342735.

Borg, L.E., and Clynne, M.A., 1998, The petrogenesis of felsic calc-alkaline magmas from the southernmost Cascades, California: Origin by partial melting of basaltic lower crust: Journal of Petrology, v. 39, p. 1197–1222, doi:10.1093/petrology/39.6.1197.

Borg, L.E., Clynne, M.A., and Bullen, T.D., 1997, The variable role of slab-derived fluids in the generation of a suite of primitive calc-alkaline lavas from the southernmost Cascades, California: Canadian Mineralogist, v. 35, p. 425–452.

Borg, L.E., Brandon, A.D., Clynne, M.A., and Walker, R.J., 2000, Re-Os isotopic systematics of primitive lavas from the Lassen region of the Cascade arc, California: Earth and Planetary Science Letters, v. 177, p. 301–317, doi:10.1016/S0012-821X(00)00051-0.

Borg, L.E., Blichert-Toft, J., and Clynne, M.A., 2002, Ancient and modern subduction zone contributions to the mantle sources of lavas from the Lassen region of California inferred from Lu-Hf isotopic systematic: Journal of Petrology, v. 43, p. 705–723, doi:10.1093/petrology/43.4.705.

Boynton, W.V., 1984, Cosmochemistry of the rare earth elements: Meteorite studies, *in* Henderson, P., ed., Rare Earth Element Geochemistry: Amsterdam, Netherlands, Elsevier, p. 63–114.

Brach-Papa, C., Van Bocxstaele, M., Ponzevera, E., and Quétel,C.R., 2009, Fit for purpose validated method for the determination of the strontium isotopic signature in mineral water samples by multi-collector inductively coupled plasma mass spectrometry: Spectrochimica Acta Part B, v. 64, p. 229–234, doi:10.1016/j.sab.2009.01.012.

Bullen, T.D., and Clynne, M.A., 1990, Trace element and isotopic constraints on magmatic evolution at Lassen volcanic center: Journal of Geophysical Research, v. 95, p. 19,671–19,691, doi:10.1029/JB095iB12p19671.

Church, S.E., 1976, The Cascade Mountains revisited: A re-evaluation in light of new lead isotopic data: Earth and Planetary Science Letters, v. 29, p. 175–188, doi:10.1016/0012-821X(76)90037-6.

Church, S.E., and Tilton, G.R., 1973, Lead and strontium isotopic studies in the Cascade Mountains; bearing on andesite genesis: Geological Society of America Bulletin, v. 84, p. 431–454, doi:10.1130/0016-7606(1973)84<431:LASISI>2.0.CO;2.

Conrey, R.M., 2009, A petrologic overview of the Boring volcanic field, Cascade Range, USA: Geological Society of America Abstracts with Programs, v. 41, Issue 7, p. 190.

Conrey, R.M., Hooper, P.R., Larson, P.B., Chesley, J., and Ruiz, J., 2001, Trace element and isotopic evidence for two types of crustal melting beneath a High Cascade volcanic center, Mt. Jefferson, Oregon: Contributions to Mineralogy and Petrology, v. 141, p. 710–732, doi:10.1007/s004100100259.

Davis, A.S., Snavely, P.D., Jr., Gray, L.B., and Minasian, D.L., 1995, Petrology of Late Eocene Lavas Erupted in the Forearc of Central Oregon: U.S. Geological Survey Open-File Report 95-40, 58 p.

Debaille, V., Blichert-Toft, J., Agranier, A., Doucelance, R., Schiano, P., and Albarède, F., 2006, Geochemical component relationships in MORB from the Mid-Atlantic Ridge, 22–35°N: Earth and Planetary Science Letters, v. 241, p. 844–862, doi:10.1016/j.epsl.2005.11.004.

Deschamps, A., and Lallemand, S., 2003, Geodynamic setting of Izu-Bonin-Mariana boninites, *in* Larter, R.D., and Leat, P.T., eds., Intra-Oceanic Subduction Systems; Tectonic and Magmatic Processes: Geological Society of London Special Publication 219, p. 163–185.

Duncan, R.A., 1982, A captured island chain in the Coast Range of Oregon and Washington: Journal of Geophysical Research, v. 87, p. 827–837, doi:10.1029/JB087iB13p10827.

Engebretson, D.C., Cox, A., and Gordon, R.G., eds., 1985, Relative Motions between Oceanic and Continental Plates in the Pacific Basin: Geological Society of America Special Paper 206, 59 p.

Eriksson, A., 2002, Stratigraphy, Structure, and Natural Gas Potential of Tertiary Sedimentary and Volcanic Units, Clatskanie 7.5-Minute Quadrangle, Northwest Oregon [M.S. thesis]: Corvallis, Oregon State University, 215 p.

Finn, C., Phillips, W.M., and Williams, D.L., 1991, Gravity Anomaly and Terrain Maps of Washington: U.S. Geological Survey Geophysical Investigations Map GP-988, scale 1:1,000,000 and 1:500,000.

Gaffney, A.M., Blichert-Toft, J., Nelson, B.K., Bizzarro, M., Rosing, M., and Albarède, F., 2007, Constraints on source-forming processes of West Greenland kimberlites inferred from Hf-Nd isotope systematics: Geochimica et Cosmochimica Acta, v. 71, p. 2820-2836.

Geist, D., and Richards, M., 1993, Origin of the Columbia Plateau and Snake River Plain: Deflection of the Yellowstone plume: Geology, v. 21, p. 789–792, doi:10.1130/0091-7613(1993)021<0789:OOTCPA>2.3.CO;2.

Gill, J.B., 1981, Orogenic Andesites and Plate Tectonics: Berlin, Springer Verlag, 401 p.

Gorring, M.L., and Kay, S.M., 2001, Mantle processes and sources of Neogene slab window magmas from Southern Patagonia, Argentina: Journal of Petrology, v. 42, p. 1067–1094, doi:10.1093/petrology/42.6.1067.

Grove, T.L., Parman, S.W., Bowring, S.A., Price, R.C., and Baker, M.B., 2002, The role of an H_2O-rich fluid component in the generation of primitive basaltic andesites and andesites from the Mt. Shasta region, N. California: Contributions to Mineralogy and Petrology, v. 142, p. 375–396, doi:10.1007/s004100100299.

Haeussler, P.J., Bradley, D.W., Goldfarb, R., Snee, L., and Taylor, C., 2003, Life and death of the Resurrection plate: Evidence for its existence and subduction in the northeastern Pacific in Paleocene-Eocene time: Geological Society of America Bulletin, v. 115, p. 867–880, doi:10.1130/0016-7606(2003)115<0867:LADOTR>2.0.CO;2.

Halliday, A.N., Fallick, A.E., Dickin, A.P., Mackenzie, A.B., Stephens, W.E., and Hildreth, W., 1983, The isotopic and chemical evolution of Mount St. Helens: Earth and Planetary Science Letters, v. 63, p. 241–256, doi:10.1016/0012-821X(83)90040-7.

Hamelin, B., and Allegre, C.J., 1985, Large-scale regional units in the depleted upper mantle revealed by an isotope study of the South-West Indian Ridge: Earth and Planetary Science Letters, v. 62, p. 341–438.

Hanan, B.B., and Graham, D.W., 1996, Lead and helium evidence from oceanic basalts for a common deep source of mantle plumes: Science, v. 272, p. 991–995, doi:10.1126/science.272.5264.991.

Harkins, S.A., Appold, M.S., Nelson, B.K., Brewer, A.M., and Groves, I.M., 2008, Lead isotope constraints on the origin of nonsulfide zinc and sulfide zinc-lead deposits in the Flinders Ranges, South Australia: Economic Geology, v. 103, p. 353–364.

Hart, S.R., 1984, A large-scale isotope anomaly in the Southern Hemisphere mantle: Nature, v. 309, p. 753–757, doi:10.1038/309753a0.

Hegner, E., and Tatsumoto, M., 1987, Pb, Sr, Nd isotopes in basalts and sulfides from the Juan de Fuca Ridge: Journal of Geophysical Research, v. 92, p. 11,380–11,386, doi:10.1029/JB092iB11p11380.

Henriksen, D.A., 1956, Eocene Stratigraphy of the Lower Cowlitz River–Eastern Willapa Hills Area, Southwestern Washington: Washington Division of Mines and Geology Bulletin 43, 122 p.

Hirschmann, M.M., and Stolper, E.M., 1996, A possible role for garnet pyroxenite in the origin of the “garnet signature” in MORB: Contributions to Mineralogy and Petrology, v. 124, p. 185–208, doi:10.1007/s004100050184.

Hole, M.J., Kempton, P.D., and Millar, L.L., 1993, Trace-element and isotopic characteristics of small-degree melts of the asthenosphere: Evidence from the alkali basalts of the Antarctic Peninsula: Chemical Geology, v. 109, p. 51–68, doi:10.1016/0009-2541(93)90061-M.

Irvine, T.N., and Baragar, W.R.A., 1971, A guide to the chemical classification of the common volcanic rocks: Canadian Journal of Earth Sciences, v. 8, p. 523–548, doi:10.1139/e71-055.

Jicha, B.R., Hart, G.L., Johnson, C.M., Hildreth, W., Beard, B.L., Shirey, S.B., and Valley, J.W., 2009, Isotopic and trace element constraints on the petrogenesis of lavas from the Mount Adams volcanic field, Washington: Contributions to Mineralogy and Petrology, v. 157, p. 189–207, doi:10.1007/s00410-008-0329-6.

Johnston, S.T., and Thorkelson, D.J., 2000, Continental flood basalts; episodic magmatism above long-lived hot spots: Earth and Planetary Science Letters, v. 175, p. 247–256, doi:10.1016/S0012-821X(99)00293-9.

Kellogg, J.B., Jacobsen, S.B., and O'Connell, R.J., 2007, Modeling lead isotopic heterogeneity in mid-ocean ridge basalts: Earth and Planetary Science Letters, v. 262, p. 328–342, doi:10.1016/j.epsl.2007.06.018.

Kenitz, S., 1997, Correlation of Volcanic Rocks within the Middle-Upper Eocene (Narizian Stage) Sedimentary Rocks in the Mist Gas Field Area, Columbia County, Oregon [M.S. thesis]: Portland, Oregon, Portland State University, 70 p.

Kimura, J., Stern, R.J., and Yoshida, T., 2005, Reinitiation of subduction and magmatic responses in SW Japan during Neogene time: Geological Society of America Bulletin, v. 117, p. 969–986, doi:10.1130/B25565.1.

Kleibacker, D.W., 2001, Sequence Stratigraphy and Lithofacies of the Middle Eocene Upper McIntosh and Cowlitz Formations, Geology of the Grays River Volcanics, Castle Rock–Germany Creek Area, Southwest Washington [M.S. thesis]: Corvallis, Oregon, Oregon State University, 215 p.

LeBas, M.J., LeMaitre, R.W., Streckeisen, A., and Zanettin, B., 1986, A chemical classification of volcanic rocks based on the total alkali silica diagram: Journal of Petrology, v. 27, p. 745–750.

Lee, C.A., Luffi, P., Plank, T., Dalton, H., and Leeman, W., 2009, Constraints on the depths and temperatures of basaltic magma generation on Earth and other terrestrial planets using new thermobarometers for mafic magmas: Earth and Planetary Science Letters, v. 279, p. 20–33, doi:10.1016/j.epsl.2008.12.020.

Leeman, W.P., Smith, D.R., Hildreth, W., Palacz, Z., and Rogers, N., 1990, Compositional diversity of late Cenozoic basalts in a transect across the southern Washington Cascades: Implications for subduction zone magmatism: Journal of Geophysical Research, v. 95, no. B12, p. 19,561–19,582, doi:10.1029/JB095iB12p19561.

Leeman, W.P., Tonarini, S., Chan, L.H., and Borg, L., 2004, Boron and lithium isotopic variation in a hot subduction zone, the southern Washington Cascades: Chemical Geology, v. 212, p. 101–124, doi:10.1016/j.chemgeo.2004.08.010.

LeRoux, A.P., Dick, H.J.B., Erlank, A.J., Reid, A.M., Frey, F.A., and Hart, S.R., 1983, Geochemistry, mineralogy, and petrogenesis of lavas erupted along the Southwest Indian Ridge between the Bouvet triple junction and 11 degrees east: Journal of Petrology, v. 24, p. 267–318.

Livingston, V.E., 1966, Geology and Mineral Resources of the Kelso-Cathlamet Area, Cowlitz and Wahkiakum Counties, Washington: Washington Division of Mines and Geology Bulletin 54, 110 p.

MacPherson, C.G., and Hall, R., 2001, Tectonic setting of Eocene boninite magmatism in the Izu-Bonin-Mariana forearc: Earth and Planetary Science Letters, v. 186, p. 215–230, doi:10.1016/S0012-821X(01)00248-5.

Madsen, J.K., Thorkelson, D.J., Friedman, R.M., and Marshall, D.D., 2006, Cenozoic to Recent plate configurations in the Pacific Basin: Ridge subduction and slab window magmatism in western North America: Geosphere, v. 2, p. 11–34, doi:10.1130/GES00020.1.

Magill, J., Cox, A., and Duncan, R., 1981, Tillamook volcanic series: Further evidence for tectonic rotation of the Oregon Coast Range: Journal of Geophysical Research, v. 86, p. 2953–2970, doi:10.1029/JB086iB04p02953.

McCutcheon, M.S., 2003, Stratigraphy and Sedimentology of the Middle Eocene Cowlitz Formation and Adjacent Sedimentary and Volcanic Units in the Longview-Kelso Area, Southwest Washington [M.S. thesis]: Corvallis, Oregon, Oregon State University, 346 p.

Moothart, S.R., 1992, Geology of the Middle and Upper Eocene McIntosh Formation and Adjacent Volcanic and Sedimentary Rock Units, Willapa Hills, Pacific County, Southwestern Washington [M.S. thesis]: Corvallis, Oregon, Oregon State University, 265 p.

Morris, J., and Hart, S.R., 1983, Isotopic and incompatible element constraints on the genesis of island arc volcanics from Cold Bay and Amak Island, Aleutians, and implications for mantle structure: Geochimica et Cosmochimica Acta, v. 47, p. 2015–2030, doi:10.1016/0016-7037(83)90217-X.

Morris, J., Leeman, W.P., and Tera, F., 1990, The subducted component in island arc lavas: Constraints from Be isotopes and B-Be systematics: Nature, v. 344, p. 31–36, doi:10.1038/344031a0.

Mullen, E.D., 1983, $MnO/TiO_2/P_2O_5$—A minor element discriminant for basaltic rocks of oceanic environments and its implications for petrogenesis: Earth and Planetary Science Letters, v. 62, p. 53–62, doi:10.1016/0012-821X(83)90070-5.

Mumford, D.F., 1988, Geology of the Elsie–Lower Nehalem River Area, South-Central Clatsop and Northernmost Tillamook Counties, Northwestern Oregon [M.S. thesis]: Corvallis, Oregon, Oregon State University, 392 p.

Nakamura, E., Ishikawa, T., Birck, J.-L., and Allegre, C.J., 1992, Precise boron isotopic analysis of natural rock samples using a boron-mannitol complex: Chemical Geology, v. 94, p. 193–204, doi:10.1016/S0009-2541(10)80004-X.

Nelson, B.K., 1995, Fluid flow in subduction zones: Evidence from neodymium and strontium isotope variations in metabasalts of the Franciscan Complex, California: Contributions to Mineralogy and Petrology, v. 119, p. 247-262.

Nielsen, R.L., Davidson, P.M., and Grove, T.L., 1988, Pyroxene-melt equilibria: An updated model: Contributions to Mineralogy and Petrology, v. 100, p. 361–373, doi:10.1007/BF00379745.

Niem, A.R., and Niem, W.A., 1984, Cenozoic geology and geologic history of western Oregon, *in* Kulm, L.D., et al., eds., Atlas of the Ocean Margin Drilling Program, Western Oregon-Washington, Continental Margin and Adjacent Ocean Floor, Region V, Ocean Margin Drilling Program Regional Atlas Series, Atlas 1: Woods Hole, Massachusetts, Marine Science International, Sheets 17 and 18.

Niem, A.R., MacLeod, N.S., Snavely, P.D., Jr., Huggins, D., Fortier, J.D., Meyer, H.J., Seeling, A., and Niem, W.A., 1992a, Offshore-Onshore Geologic Cross Section, Northern Oregon Coast Range to Continental Slope: Oregon Department of Geology and Mineral Industries Continental Margin Transect OGI-26, 10 p.

Niem, W.A., Niem, A.R., and Snavely, P.D., Jr., 1992b, Early and Mid-Tertiary oceanic realm and continental margin—Western Washington-Oregon coastal sequence, *in* Burchfiel, B.C., Lipman, P.W., and Zoback, M.L., eds., The Cordilleran Orogen: Conterminous U.S.: Boulder, Colorado, Geological Society of America, The Geology of North America, v. G-3, p. 265–270.

Obrebski, M., Allen, R.M., Xue, M., and Hung, S.-H., 2010, Slab/plume interaction beneath the Pacific Northwest: Geophysical Research Letters, v. 37, p. L14305, doi:10.1029/2010GL043489.

Oxford, J., 2006, Early Oligocene Intrusions in the Central Coast Range of Oregon: Petrography, Geochemistry, Geochronology, and Implications for the Tertiary Magmatic Evolution of the Cascadia Forearc [M.S. thesis]: Corvallis, Oregon, Oregon State University, 250 p.

Parker, D.F., Hodges, F.N., Perry, A., Mitchener, M.E., Barnes, M.A., and Ren, M., 2010, Geochemistry and petrology of late Eocene Cascade Head and Yachats basalt and alkali intrusions of the Oregon Coast Range, USA: Journal of Volcanology and Geothermal Research, v. 198, p. 311–324, doi:10.1016/j.jvolgeores.2010.09.016.

Payne, C.W., 1998, Lithofacies, Stratigraphy, and Geology of the Middle Eocene Type Cowlitz Formation and Associated Volcanic and Sedimentary Units, Eastern Willapa Hills, Southwest Washington [M.S. thesis]: Corvallis, Oregon, Oregon State University, 235 p.

Pearce, J.A., and Norry, M.L., 1979, Petrogenetic implications of Ti, Zr, Y, and Nb variations in volcanic rocks: Contributions to Mineralogy and Petrology, v. 25, p. 956–983.

Phillips, W.M., 1987, Geologic Map of the Mt. St. Helens Quadrangle, Washington: Washington Division of Geology and Earth Resources Open-File Report 87-4, scale 1:100,000, 1 sheet, 63 p. text.

Phillips, W.M., Walsh, T.J., and Hagen, R.A., 1989, Eocene transition from oceanic to arc volcanism, southwest Washington: U.S. Geological Survey Open-File Report 89–178, p. 199–256.

Prytulak, J., Vervoort, J.D., Plank, T., and Yu, C., 2006, Astoria Fan sediments, DSDP Site 174, Cascadia Basin: Hf-Nd-Pb constraints on provenance and outburst flooding: Chemical Geology, v. 233, p. 276–292, doi:10.1016/j.chemgeo.2006.03.009.

Pyle, D.G., Hanan, B.B., Graham, D.W., and Duncan, R.A., 1997, Siletzia; geochemistry and geochronology of the Yellowstone hot spot volcanism in a suboceanic setting: Geological Society of America Abstracts with Programs, v. 29, Issue 6, p. 298.

Pyle, D.G., Duncan, R., Wells, R.E., Graham, D.W., Harrison, B., and Hanan, B., 2009, Siletzia: An oceanic large igneous province in the Pacific Northwest: Geological Society of America Abstracts with Programs, v. 41, no. 7, p. 369.

Rarey, P.J., 1985, Geology of the Hamlet–North Fork of the Nehalem River Area, Southern Clatsop and Northernmost Tillamook Counties, Northwest Oregon [M.S. thesis]: Corvallis, Oregon, Oregon State University, 457 p.

Ryan, J.G., Leeman, W.P., Morris, J.D., and Langmuir, C.H., 1996a, The boron systematics of intraplate lavas: Implications for crust and mantle evolution: Geochimica et Cosmochimica Acta, v. 60, p. 415–422, doi:10.1016/0016-7037(95)00402-5.

Ryan, J.G., Morris, J., Bebout, G.E., and Leeman, W.P., 1996b, Describing chemical fluxes in subduction zones: Insights from "depth-profiling" studies of arc and forearc rocks, *in* Bebout, G.E., Scholl, D., Kirby, S., and Platt, J., eds., Subduction Top to Bottom: American Geophysical Union Monograph 96, p. 263–268.

Safley, L.E., 1989, Geology of the Rock Creek–Green Mountain Area, Southeast Clatsop and Northmost Tillamook Counties, Northwest Oregon [M.S. thesis]: Corvallis, Oregon, Oregon State University, 262 p.

Schmidt, M.E., Grunder, A.L., and Rowe, M.C., 2008, Segmentation of the Cascade arc as indicated by Sr and Nd isotopic variation among diverse primitive basalts: Earth and Planetary Science Letters, v. 266, p. 166–181.

Schoonmaker, A., Kidd, W.S.F., and Bradley, D.C., 2005, Foreland-forearc collisional granitoid and mafic magmatism caused by lower-plate lithospheric slab breakoff; the Acadian of Maine, and other orogens: Geology, v. 33, p. 961–964, doi:10.1130/G21832.1.

Simpson, R.W., and Cox, A., 1977, Paleomagnetic evidence for tectonic rotation of the Oregon Coast Range: Geology, v. 5, p. 585–589, doi:10.1130/0091-7613(1977)5<585:PEFTRO>2.0.CO;2.

Smith, D.R., and Leeman, W.P., 1987, Petrogenesis of Mount St. Helens dacitic magmas: Journal of Geophysical Research, v. 92, p. 10,313–10,334, doi:10.1029/JB092iB10p10313.

Snavely, P.D., Jr., 1987, Tertiary geologic framework, neotectonics, and petroleum potential of the Oregon-Washington continental margin, *in* Scholl, D.W., and Grantz, A., eds., Western North America and Adjacent Ocean Basins—Beaufort Sea to Baja California: Circum-Pacific Council for Energy and Mineral Resources, Earth Sciences Series, v. 6, p. 305–335.

Snavely, P.D., Jr., and Wells, R.E., 1996, Cenozoic evolution of the continental margin of Oregon and Washington, *in* Walsh, T.J., Kockelman, W.J., and Priest, G.R., eds., Assessing Earthquake Hazards and Reducing Risk in the Pacific Northwest, Volume 1: U.S. Geological Survey Professional Paper 1560, p. 161–182.

Sun, S., and McDonough, W.F., 1989, Chemical and isotopic systematic of oceanic basalts: Implications for mantle composition and processes, *in* Saunders, A.D., and Norry, M.J., eds., Magmatism in the Ocean Basins: Geological Society of London Special Publication 42, p. 313–345.

Takahashi, E., Shimazaki, T., Txuzaki, Y., and Yoshida, H., 1993, Melting study of a peridotite KLB-1 to 6.5 GPa, and the origin of basaltic magmas: Philosophical Transactions of the Royal Society of London, v. 342, p. 105–120.

Tepper, J.H., Clark, K., Asmerom, Y., and McIntosh, W., 2004, Eocene adakites in the Cascadia forearc: Implications for the position of the Kula-Farallon Ridge: Geological Society of America Abstracts with Programs, v. 36, no. 4, p. 69.

Tepper, J.H., Nelson, B.K., Clark, K., and Barnes, R.P., 2008, Heterogeneity in mantle sources for Eocene basalts in Washington: Trace element and Sr-Nd isotopic evidence from the Crescent and Teanaway basalts [abs.]: Eos (Transactions, American Geophysical Union), v. 89, abstract V41D–2121.

Thorkelson, D.J., Madsen, J.K., and Slugett, C.L., 2011, Mantle flow through the Northern Cordilleran slab window revealed by volcanic geochemistry: Geology, v. 39, p. 267–270, doi:10.1130/G31522.1.

Trehu, A.M., Asudeh, I., Brocher, T.M., Luetgert, J.H., Mooney, W.D., Nabelek, J.L., and Nakamura, Y., 1994, Crustal structure of the Cascadia forearc: Science, v. 266, p. 237–243, doi:10.1126/science.266.5183.237.

Ulmer, P., 1989, The dependence of the Fe^{2+}-Mg cation-partitioning between olivine and basaltic liquid on pressure, temperature and composition; an experimental study to 30 kbars: Contributions to Mineralogy and Petrology, v. 101, p. 261–273, doi:10.1007/BF00375311.

Verplanck, E.P., and Duncan, R.A., 1987, Temporal variations in plate convergence and eruption rates in the western Cascades, Oregon: Tectonics, v. 6, p. 197–209, doi:10.1029/TC006i002p00197.

Walker, G.W., and MacLeod, N.S., 1991, Geologic map of Oregon: U.S. Geological Survey, scale 1:500,000, 2 sheets.

Walsh, T.J., Korosec, M.A., Phillips, W.M., Logan, R.L., and Schasse, H.W., 1987, Geologic Map of Washington, Southwest Quadrant: Washington Division of Geology and Earth Resources Geologic Map GM-34, scale 1:250,000, 2 sheets, 28 p. text.

Wells, R.E., 1981, Geologic Map of the Eastern Willapa Hills, Cowlitz, Lewis, Pacific, and Wahkiakum Counties, Washington: U.S. Geological Survey Open-File Report 81-674, scale 1:62,500.

Wells, R.E., 2007, Reconsidering the origin and emplacement of Siletzia: Geological Society of America Abstracts with Programs, v. 39, no. 4, p. 19.

Wells, R.E., and Coe, R.S., 1985, Paleomagnetism and geology of Eocene volcanic rocks of southwest Washington, implications for mechanisms of tectonic rotation: Journal of Geophysical Research, v. 90, no. B2, p. 1925–1947, doi:10.1029/JB090iB02p01925.

Wells, R.E., Engebretson, D.C., Snavely, P.D., Jr., and Coe, R.S., 1984, Cenozoic plate motions and the volcano-tectonic evolution of western Oregon and Washington: Tectonics, v. 3, p. 275–294, doi:10.1029/TC003i002p00275.

White, W.M., Hofmann, A.W., and Puchelt, H., 1987, Isotope geochemistry of Pacific mid-ocean ridge basalt: Journal of Geophysical Research, v. 92, p. 4881–4893, doi:10.1029/JB092iB06p04881.

Wolfe, E.W., and McKee, E.H., 1968, Geology of the Grays River Quadrangle, Wahkiakum and Pacific Counties, Washington: Washington Division of Mines and Geology Geologic Map GM-4, scale 1:62,500.

Wolfe, M.R., and Tepper, J.H., 2004, Felsic volcanic rocks on the Olympic Peninsula and their implications for ridge subduction: Geological Society of America Abstracts with Programs, v. 36, no. 5, p. 223.

Wyllie, P.J., 1981, Plate tectonics and magma genesis: Geologische Rundschau, v. 70, p. 128–153, doi:10.1007/BF01764318.

Science Editor: Christian Koeberl
Associate Editor: Sandra M. Barr

Manuscript Received 25 July 2011
Revised Manuscript Received 21 November 2011
Manuscript Accepted 29 November 2011

Printed in the USA